Ebert-Fastie Spectral Response Measurements and Simulation

A Thesis
SUBMITTED TO THE FACULTY OF
UNIVERSITY OF MINNESOTA
BY

Aaron Smith

IN PARTIAL FULFILLMENT OF THE REQUIREMENTS
FOR THE DEGREE OF
MASTER OF SCIENCE

Shaul Hanany

May 2014

Acknowledgements

I thank my friends and family for all of their support throughout the years as well as those I have worked with for teaching me so much.

Dedication

To those who have helped me through the good times and the bad.

Abstract

We investigated the behavior of an Ebert-Fastie spectrometer using reflected ruled diffraction gratings in the 150-410 GHz band for calibration of the E and B EXperiment (EBEX). This behavior is modeled with the simulation software PCgrate. Comparisons show that the experimental and simulated results had significant differences.

Table of Contents

List of Tables

List of Figures

1. Introduction

The E and B EXperiment (EBEX) is a balloon based experiment that uses an array of super conducting bolometers to make measurements of the cosmic microwave background. The goal of this exploration is to determine the spectral response of the Ebert-Fastie spectrometer used in calibrating EBEX. The spectral response of the Ebert-Fastie and EBEX have been measured over a frequency band between 90 GHz and 510 GHz. The goal of this exploration is to determine the response of the Ebert-Fastie alone, allowing for the response of the EBEX bolometers to be determined from the previous experiment.

This is done using the program PCgrate coupled with experimental measurements using a different detector than EBEX. Comparison between the two sets of experimental data would provide information about the spectral response of the detectors in EBEX, while the simulation acts as a secondary check on both sets of measurements. The experimental measurements were conducted with a silicone bolometer that is expected to have a flat response over the frequencies of light that we are interested in measuring. Since the response of the silicone bolometer is assumed to be constant on our frequency range, any structure when measuring the response of the Ebert-Fastie should be from the Ebert-Fastie itself. This structure can be removed from the measurements made by EBEX to leave only the response of the EBEX detectors. PCgrate provided simulations that were analyzed to provide efficiency curves of the system used in

the experimental measurements. These simulations act as a secondary check on the experiment being done.

2. Hardware

The system is designed to use an Ebert-Fastie spectrometer to mechanically separate frequencies of light. The design makes use of a single spherical mirror opposite a diffraction grating as seen in Figure 1.1. Light enters through an entrance aperture, placed at the focal length of the spherical mirror and is then reflected off the mirror onto the

grating where the light is reflected at different angles depending on frequency. Only the frequency of light reflected at the same angle as the incident angle relative to the mirror is properly reflected by the spherical mirror into the exit

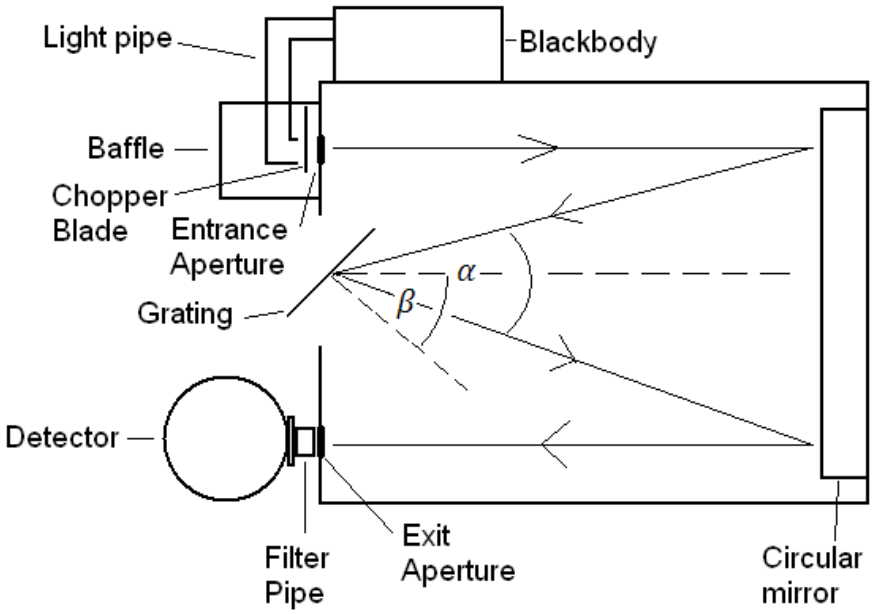

Figure 2.1: Outline of the Ebert-Fastie setup used in the EBEX calibration. The blackbody acts as a source of light that is reflected into the system through a light pipe and chopper blade. This chopped light is reflected by the spherical mirror onto the diffraction grating where it is separated based off frequency. This separated light is reflected off the mirror again and is detected by the detector.

aperture. This light is then measured by some detector

The system used for the EBEX calibration makes use of an Infrared Industries cavity blackbody reference source that operates at 1000°C to create a light

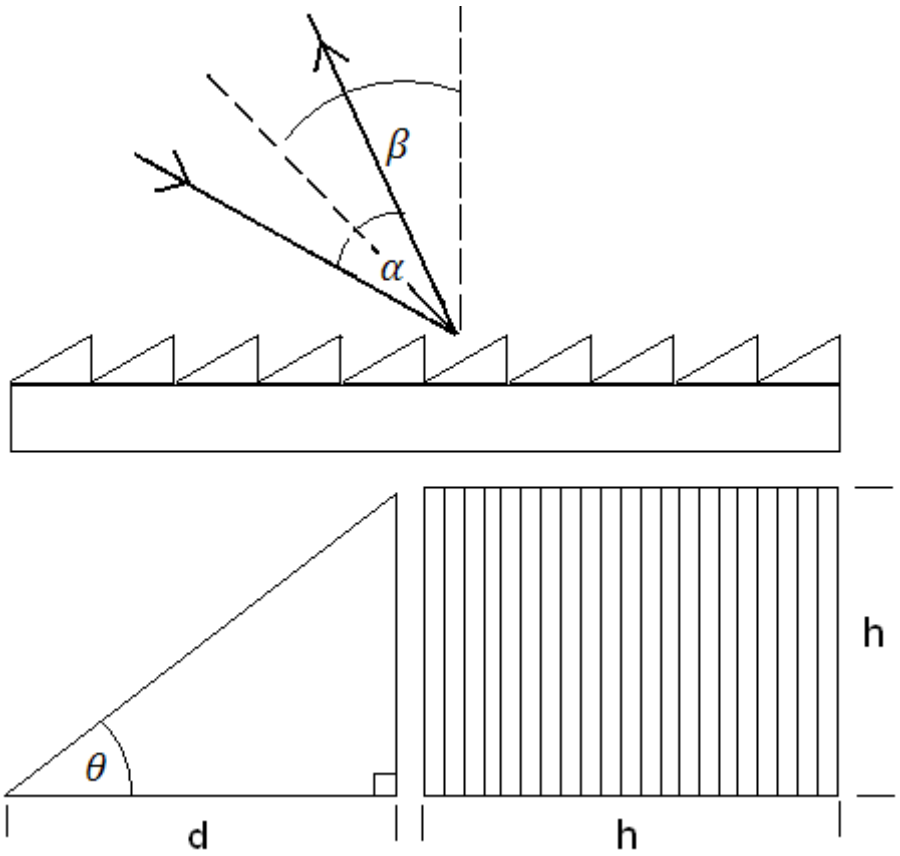

Figure 2.2: Diagram of blazed diffraction gratings used. These gratings used a 30° blazed angle on a right triangle, repeated over a square. The values for the given parameters are given in Table 1.

source for the Ebert-Fastie. This light is turned 180° by a brass light pipe and positioned between a chopper blade and the entrance aperture. This source provides significant signal at each of the desired frequency bands. These bands peak at 150 GHz, 250 GHz, and 410 GHz, and the combined band extends between 90 and 510 GHz.

The chopper blade provides a consistent chopped signal. This signal fluctuates based on the amount of light blocked by the chopper blade. The signal max is when the neither of the chopper blade's two blades intercept the light from the light pipe. The signal is at a minimum when the chopper blade covers the light pipe completely. This is used later with a lock-in amplifier to increase the signal to noise ratio.

The leaked chopped signal is reduced by use of Eccosorb LS- 30 at various locations. This absorbing material is placed on the chopper blade facing the light pipe to reduce reflections when the signal is to be minimized. S baffle is also in place to minimize these reflections from leaking into the detector. The baffle is made up of one layer of aluminum foil, one of cardboard, and a final layer of Eccosorb LS-30. Eccosorb HR-10 is placed on the interior of the Ebert-Fastie to minimize reflection from the aluminum walls of the box.

h=150mm
α=17.86˚
θ=30˚
d=4mm (150 GHz)
d=2.4mm (250 GHz)
d=1.5mm (410 GHz)
β=variable

Table 1: Listed are the parameters for the gratings used for the Ebert-Fastie setup seen in Figure 2. The periods for each of the three gratings are different depending on which frequency band is being investigated.

Once the light enters the Ebert-Fastie it reflects off the aluminum spherical mirror and illuminates one of the three possible diffraction gratings. The gratings used are aluminum echelette gratings blazed at a θ=30° angle, as seen in Figure 1.2. The period of the grating, d, depends on the peak frequency desired. The grating base is made up of a square aluminum base. During operation the

grating is turned to some angle β which selects the incident angle of the light and thus the frequencies measured. Only light reflected at an angle of β-α/2 is properly reflected off the spherical mirror into the exit aperture. The angle of the reflected light depends on the angle of the incident light, the period of the grating d, the wavelength of the incident light λ, and the reflected order n, as seen in equation 1 below. The separate of light allows for a specific choice of frequency.

(Eq 1.) $$sin(\alpha/2+\beta)+sin(\alpha/2-\beta)=n\lambda/d$$

Between the exit aperture and the detector is a short aluminum light pipe surrounded by Eccosorb LS-30 that houses three filters. The first is a high pass aluminum wave guide that blocks out low frequencies of light. This is followed by two low pass filters made up of a copper mesh, these block out higher frequencies of light.

There are two of these filters to ensure that high frequency leaks at a specific frequency are at a minimum. For each band of interest, the 150 GHz, 250 GHz, and 410 GHz bands, there is a separate set of three filters (two low pass and one high pass) with the exception of the 410 GHz band which only has one low pass filter. These filters define the band width. After the light passes through the filters it reaches the detector window.

The detector used a liquid helium cooled silicone bolometer to measure power incident on the detector window. The silicone bolometer is chilled to 4.2 K by liquid helium stored in a cryostat that houses the detector. This detector is assumed to have the same response to each wavelength of light in the spectrum

of interest. The electronics also house use resistance changes in the bolometer to output a chopped signal in volts that is analyzed using a lock-in amplifier.

3. Software

Modeling of this system took place using PCgrate S 6.1 software. This software models the behavior of diffraction gratings, including reflected angle, efficiency, and polarization. This program allowed us to form a theoretical basis for understanding and predicting measurements. This software also acted as a secondary confirmation of the accuracy of the experimental measurements, as if there is a strong relationship between behavior predicted by PCgrate, and the experiment itself, more confidence can be had in the measurement.

PCgrate applies an electromagnetic theory of gratings to simulate the behavior of diffraction gratings. When applying an electromagnetic theory for gratings the general approach is to solve for the Helmholtz equation for each portion of the field solved using the grating as a boundary (Petit). This means satisfying the Helmholtz equation above and inside the grating. These can then be solved by various different numerical methods. The most popular of which is the integral method. This method expresses the field in terms of integrals that are defined along the surface of the grating. These expressions contain an unknown function, or finite series of functions, that is then determined to solve for the field itself. The most general method for establishing this problem is to make use of distribution theory, which allows for the unknown functions to be defined as the change in the field across the surface of the grating. Physically this is the surface current associated with the field for the infinity conductive material (Petit).

The well established integral method works well for infinitely conductive gratings, however breaks down when the situation is far from the ideal. PCgrate uses a modified integral method that makes use of a few tricks to achieve better numeric results for the non-ideal cases. The first alteration is redefining the incident and reflected waves as cylindrical functions instead of plane waves. Typically diffraction gratings are solved under the assumption that the surface current give rise to a plane waves, which does not allow for interference due to the periodicity of the grating with space. The second alteration in the modified method is to redefine conservation of energy using Umov-Poynting vector. This allows for energy conservation to take into account absorption of light, which had traditionally been ignored. This is especially important for gratings with several layers (Goray).

While the alterations made in the modified integral method used by PCgrate are not intended to improve the infinite conductivity case used in the simulations considered here, PCgrate did provide adequate results. Implementation of the more traditional integration method provided unsatisfactory results when compared with experimental results.

As with any theoretical model, PCgrate does not perfectly predict the behavior of physical grating measurements. There is, however, a strong correlation between the predictions made by PCgrate and physical grating measurements. When testing the validity of the program the results were compared with measurements made at Thorlabs (Thorlabs, Ruled Diffraction

Gratings) for different gratings. Figure 3.1 displays the comparison between the measured and predicted values. These measurements were done such that α=0°, also known as in Littrow. The grating in question was aluminum coated, giving a highly reflective coating for the frequencies in question. For the purposes of the simulation the surface was assumed to be a perfect conductor. The graph provides the efficiency of the reflected light compared to the incident light as a function of wavelength. It is clear the general shape of the prediction matches will with the measurement, with the peak efficiency being significantly high value for the prediction.

The primary exceptions are the sharp peaks along the contour of the curve in the predicted measurement. These features are believed to not be physically due to the discontinuity in the energy balance seen in the figure. This curve is used as a measure of quality of the simulation, as the energy balance should always be one. The sharp peaks in the energy balance correlate directly to the sharp peaks in the efficiency of the prediction, therefore it is assumed when such erratic behavior in the energy balance is present efficiency values in that region should not be trusted with the same certainty as other areas. The same trend in efficiency is seen in the appendix in Figure A1.1 and Figure A1.2 for other experimentally measured gratings.

From the experimental comparison it was concluded that PCgrate is a reasonable simulation of diffraction grating efficiency. The simulation does not

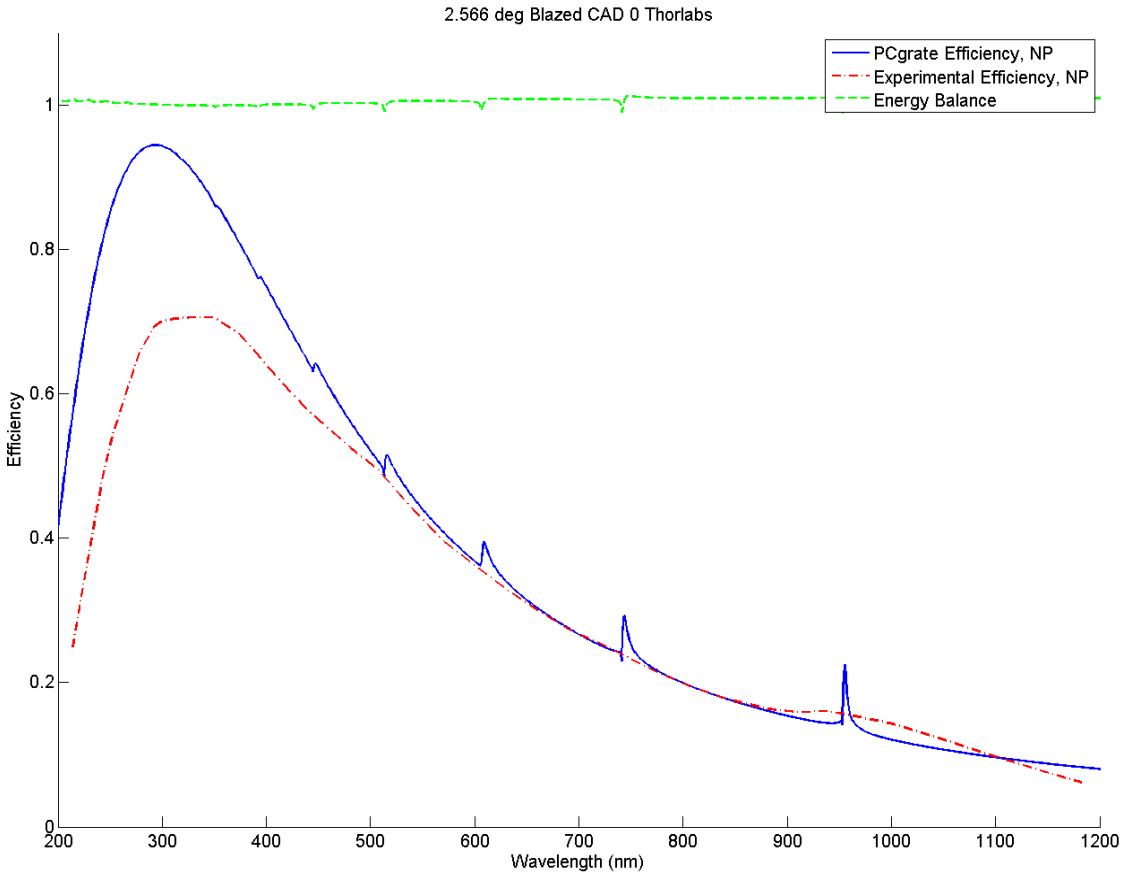

Figure 3.1: plot of the Efficiency of non-polarized (NP) for the grating for both an experimental measurement (in green) and the theoretical prediction from PCgrate (in blue). The curve in red is the energy balance from PCgrate. The grating is question is an upper right triangle with a blazed angle of 2.566° and a grove frequency of 300 groves/mm. Measurements were done in Littrow for the -1 order (Thorlabs, Ruled Diffraction Gratings).

however accurately predict all features of a diffraction grating. Analysis should thus be limited to the general trends within the efficiency curve, while overall magnitudes are assumed to vary. This knowledge was the applied in comparing simulations to experimental measurements in the Ebert-Fastie setup.

4. Simulation Results

There are three major components to the Ebert-Fastie spectral output that influence the shape of the response: the blackbody, the diffraction grating, and the high and low pass filters. The blackbody provides the base signal that is then separated by wavelength by the diffraction grating. Each wavelength of light has a different efficiency based upon the parameters of the grating. This efficiency is defined as the difference between the power incident and the power reflected for a single wavelength. This separated light is then further altered by the low and high pass filters, which also have transmission efficiencies that depend on wavelength. This filtered light is further altered by the window to the detector.

The bands of interest are centered at 150 GHz, 250 GHz, and 410 GHz. The width of each band is determined by the high and low pass filters. An example of the filters can be seen in Figure 4.1. During measurement these bands correspond to grating angles between 20 and 50 degrees.

The output of the blackbody for the 150 GHz band can be found in Figure 4.2. This is the standard blackbody spectral radiance. The frequencies of interest are well within the range where the Rayleigh-Jeans law applies, therefore the spectral radiance is proportional to the frequency squared. This influences the shape of the overall efficiency of the Ebert-Fastie, and is therefore an important factor when piecing together the expected efficiency curve shape.

The detector window is the same for each frequency measurement and has behavior shown in Figure 4.3. This curve is measured data for the high-density

polyethylene

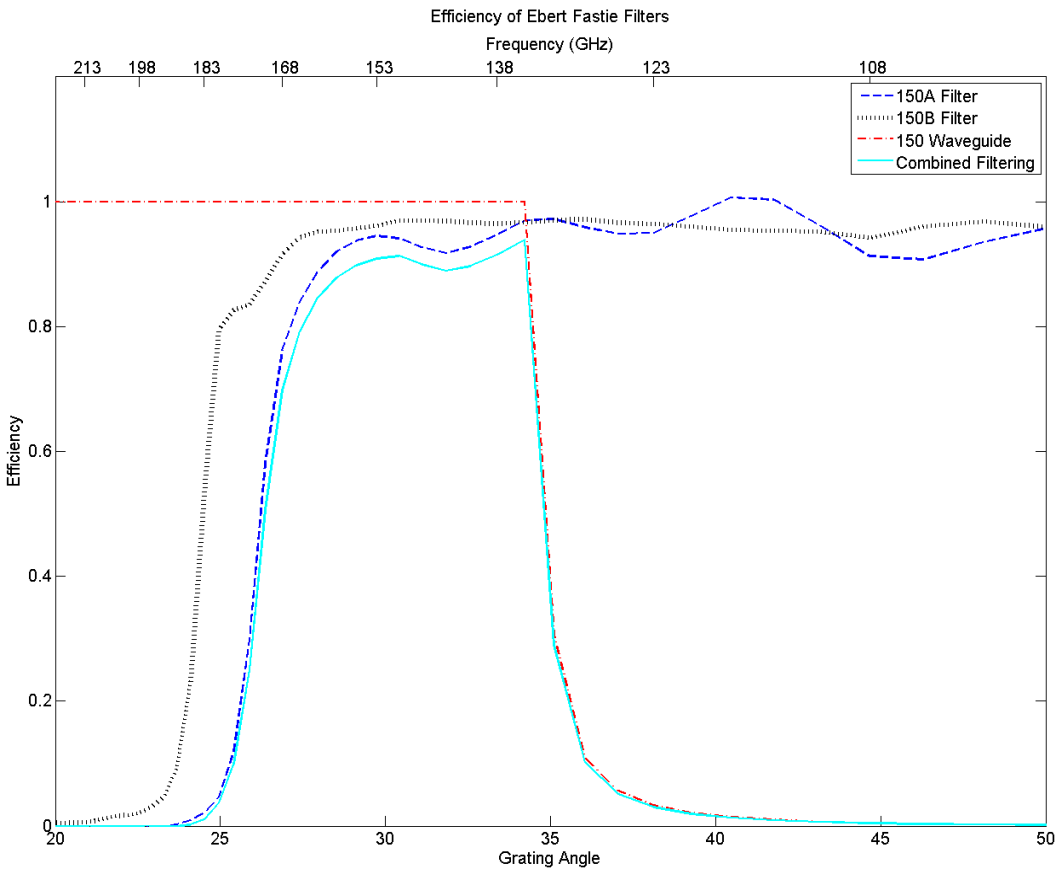

Figure 4.1: the transmission efficiency of each filter used in the 150 GHz measurement. Filters 150A and 150B are copper mesh filters, while 150 waveguide is an aluminum waveguide.

diamond coated window used in the experiment. The band of interest is at wavelengths over 1000 microns where the shape of this curve is assumed to be flat and have high transmission. The grating window can be ignored when considering lower orders. When considering higher orders, those with peaks above 20 THz, this window completely blocks the transmission of the light, allowing these higher orders to be ignored, despite the blackbody outputting much more power at higher frequencies.

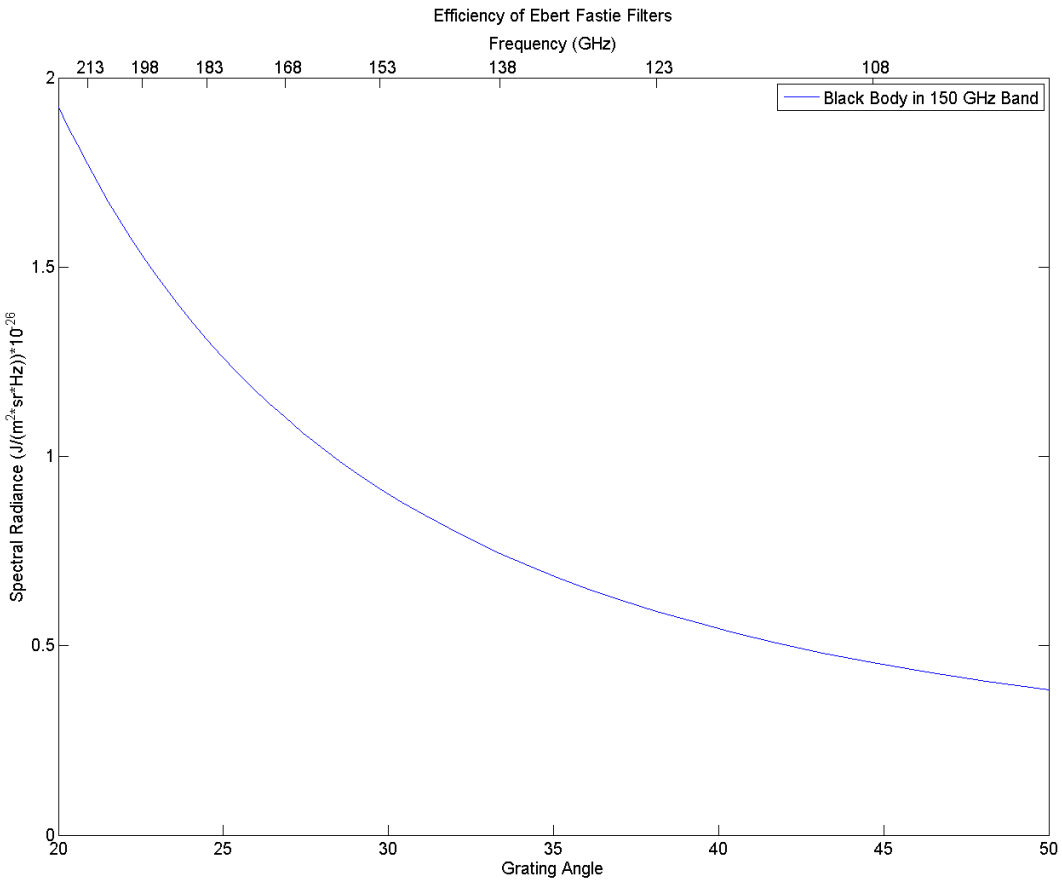

Figure 4.2: the output of the blackbody verse the grating angle used to measure that given frequency.

The spectral dependence of the 150 GHz diffraction grating for the second order (listed as -2 due to β being to the left of the perpendicular of the grating) can be found in Figure 4.4. Different gratings are used for the 250 GHz and 410 GHz measurements shown in Figure A2.1 and Figure A2.2. Gratings can have polarizing effects and therefore are shown here in terms of the reflected light polarizations, TM (perpendicular to the grating groves), and TE (parallel to the grating groves). The second order is the primary operational order of the grating by design. The period, d, and diffraction angle, θ, are such that this grating will

peak at 150 GHz while in the second order and in the Littrow configuration. This peak would be when the grating is turned to the blazed angle of 30°. The plot given in

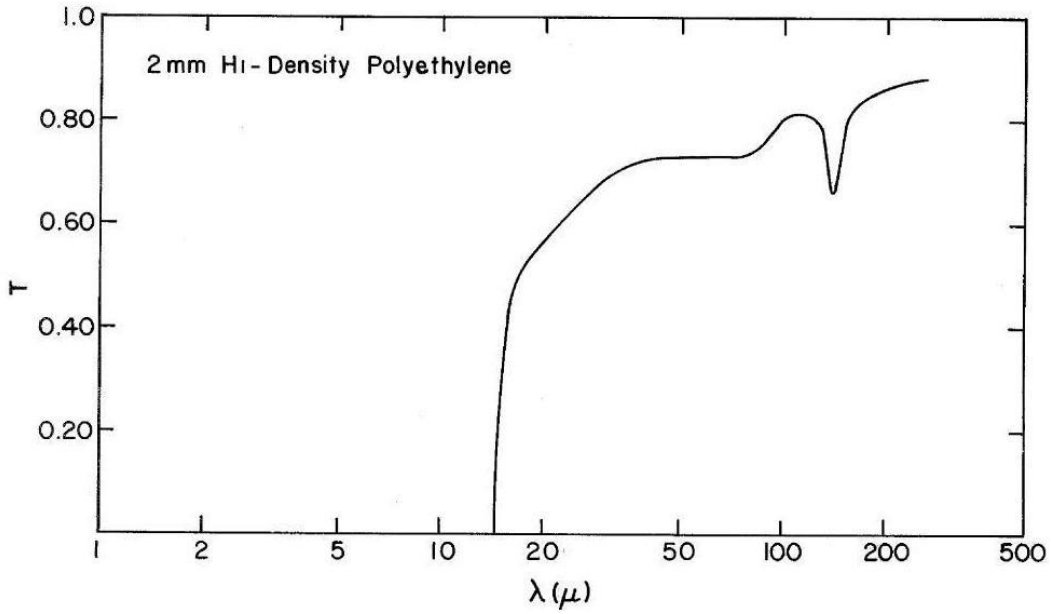

Figure 4.3: transmission of the cryostat filter window. This is assumed to be 1.0 for wavelengths greater than 1000 μm. This is a diamond dust coated hi-density polyethelene window at 300k from Infrared Laboratories.

Figure 4.4 does not peak at a grating angle of 30° due to the fact that the Ebert-Fastie works in an off Littrow configuration, where α=17.86°, not 0°. The response of the grating greatly influences the efficiency curve of the Ebert-Fastie, due to the response of the non-polarized light (NP) not having a constant response with angle.

The final piece of the puzzle when determining the spectral response of the Ebert-Fastie are the high and low pass filters. These filters are in place to select a specific range of frequencies, defining the band of operation. An example of

filters is giving in Figure 4.1 for the 150 GHz band, and Figures A2.3 and Figure A2.4 for the 250 GHz and 410 GHz filters respectively. The primary function of these filters is to eliminate light from orders other than the second order. When the grating is turned to a specific angle, fixing β, there are multiple possible reflected angles that satisfy the equation, each with a different frequency. The filters are in place to reduce or eliminate these other orders. Plots of the other orders can be found in Figure A3.1-A3.9. The orders with frequencies

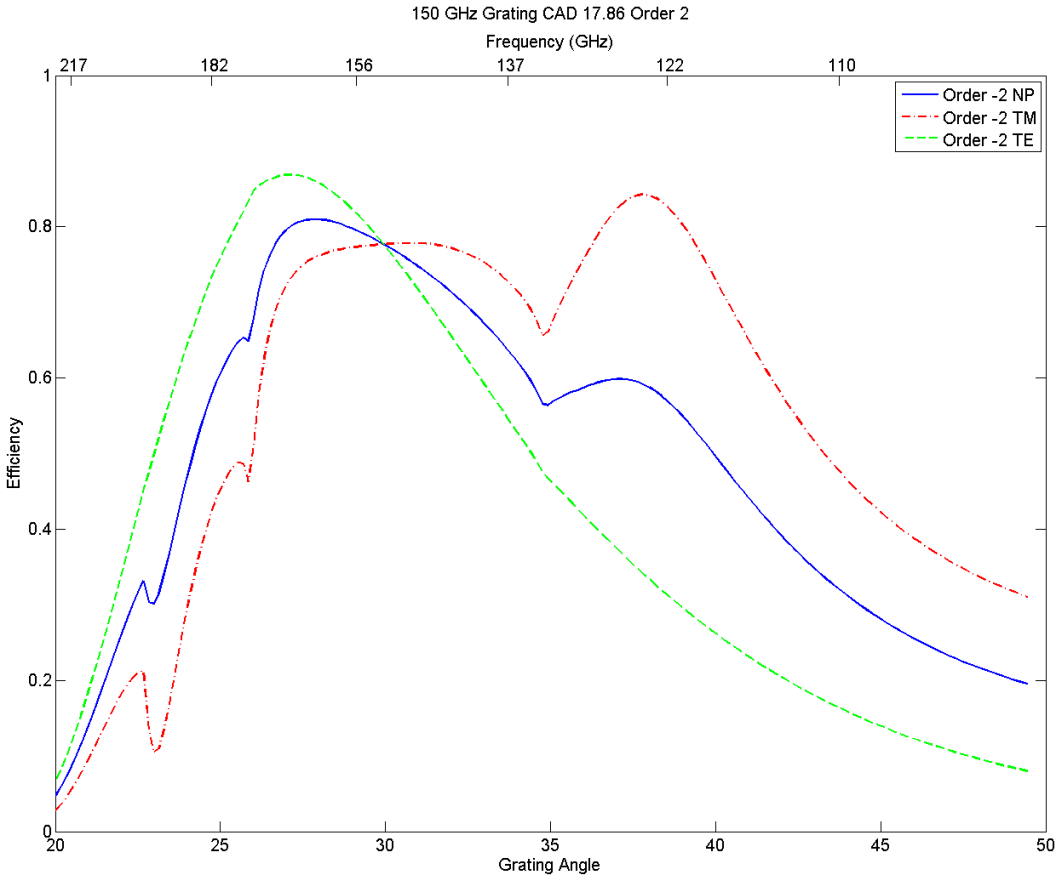

Figure 4.4: the efficiency of the 150 GHz grating. The grating is operated in the second order (-2) and is shown in terms of the polarizations. The efficiency of Order -2 TE is that of light parallel to the groves of the grating, while the TM polarization is perpendicular to the groves.

higher than 20 THz (not shown) are completely eliminated by the detector window, while lower frequency light is eliminated by the filters (signal contribution is less than 1%). This is a band between 750 GHz and 20 THz where the window does not block light and measurements for the low pass filters have not been made. Here the low pass filters were assumed to maintain the efficiency they had measured having at 750 GHz. Together the filters eliminate all orders other than the second order, and a small contribution from the first order, for the 150, 250 and 410 GHz grating.

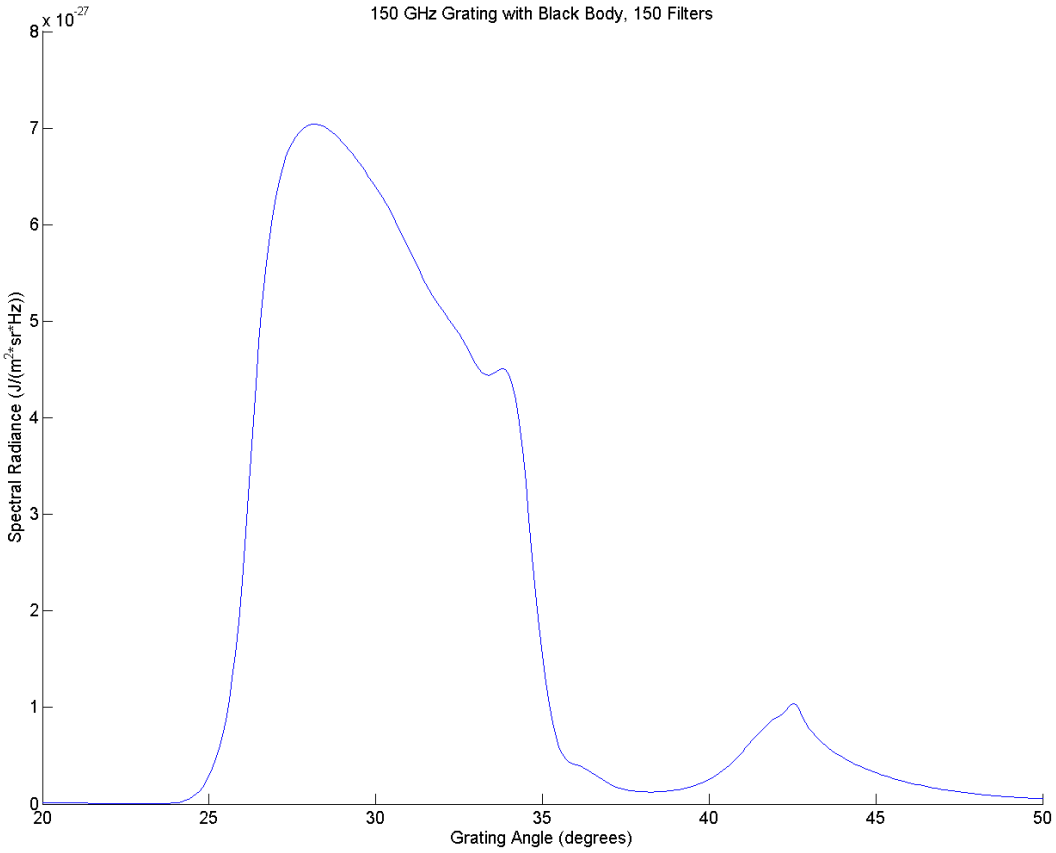

Figure 4.5: theoretical spectral response of the Ebert-Fastie including orders 1-15. This includes the blackbody, diffraction grating, high pass filters, low pass filters, and detector window.

Figure 4.5 displays the behavior of the 150 GHz measurement. In this measurement the contribution from the other orders is limited. These orders contribute to the signal between 40 and 45 degrees, but do not significantly alter the signal in the primary band between 25 and 35 degrees. Similar behavior for the 250 and 410 GHz gratings are seen in Figure A2.5 and A2.6 respectively. These represent the initial expected response of the Ebert-Fastie in normal operating conditions. The most important features common in each graph is a peak at approximately 28°, range of high signal between 25° and 35° (lower for 410 GHz), and sharp cut offs beyond the high signal range.

5. Experimental Results

The first experimental results from the Ebert-Fastie showed a flaw in the initial simulation. The low pass filters allow low frequencies to pass freely, while blocking higher frequencies of light after some cutoff point. Two filters are used in each band to help eliminate the possibility of high frequency leaks beyond this cutoff; however this proved to not be enough. Figure 5.1 shows the response of the Ebert-Fastie in standard 150 GHz operation, using the three 150 GHz filters and the 150 GHz grating.

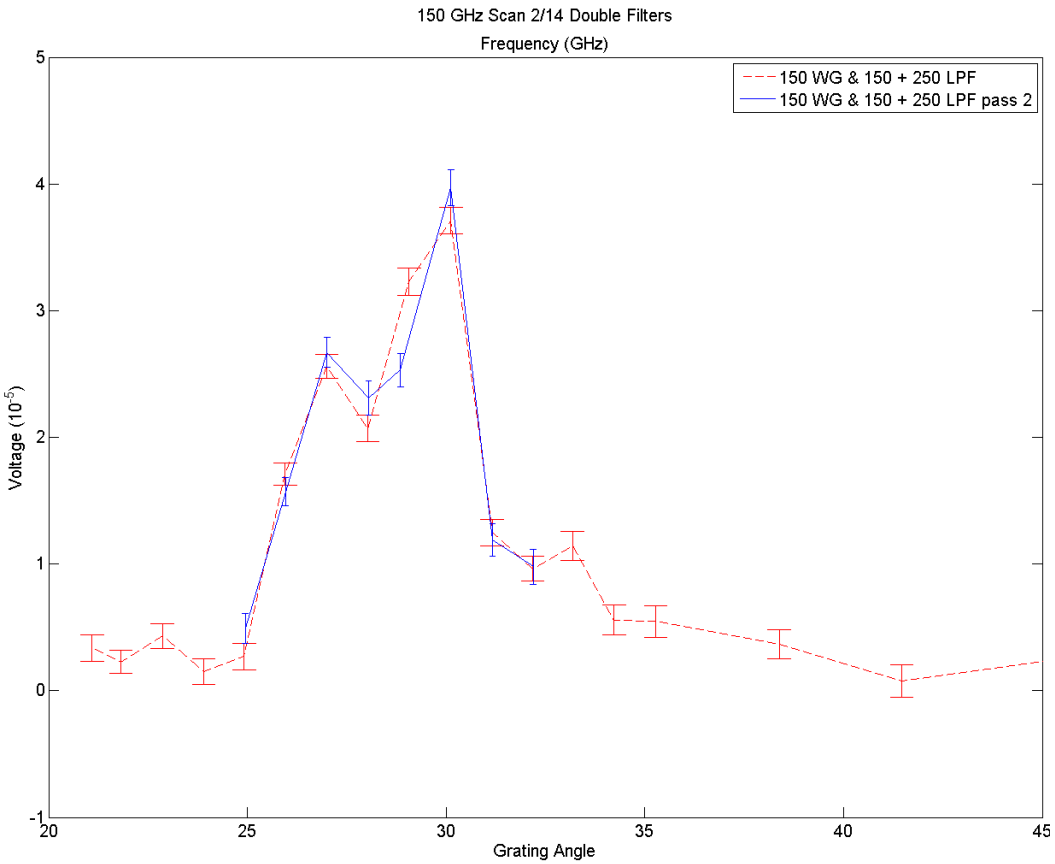

Figure 5.1: Measured response of the Ebert-Fastie using the standing 150 high pass filter (WG) and the two 150 low pass filters (LPF).

It was expected that the plots in Figure 5.1 and Figure 4.5 would peak in approximately the same locations, however the simulation peaked at 28° and the experimental results showed a clear peak at 30°. This was believed to be due to leakage of high frequency light by the low pass filters. High frequencies of light were suspected of entering the signal due to a large peak at 30°. This is because higher orders, those that reflect high frequencies of light, peak around the blazed angle of 30°, where higher orders have sharper peaks.

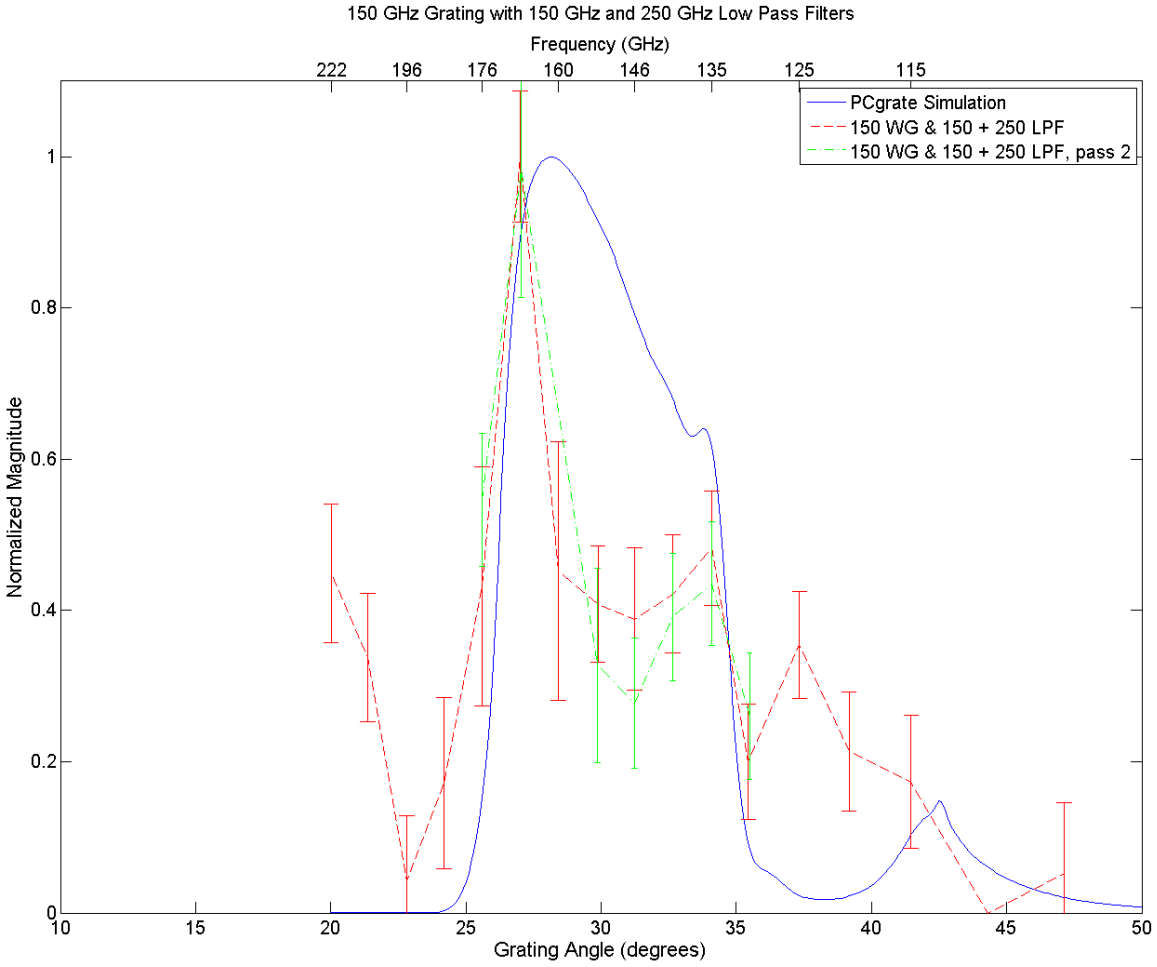

Figure 5.2: measured spectral response of the Ebert-Fastie when using two sets of low pass filters (LPF) compared to the simulated response. The response peaks at approximately 27 degrees when measured at is located at 29 degrees when simulated.

This is clearly seen in Figure A3.1-A3.9; as the order increases the angular range with significant efficiency narrows, while the peak of this range remains at the blazed angle. High orders thus can contribute significantly to the efficiency of the Ebert-Fastie, but would result in a peak around the blazed angle only.

The theory of leakage of the low pass filters was tested by adding additional low pass filters that were expected to have high and flat transmission within the band of interest. This would create no significant change in shape of the desired signal, but would reduce the change of high frequency leaks. The result of using both the 150 GHz and 250 GHz sets of filters is shown in Figure 5.2. Here the signal at 30° was reduced significantly. This implies that high frequency light was leaking into the measured signal, and is now eliminated.

Comparisons shown in Figure 5.2 show the simulated results and experimental results are not consistent. The most striking discrepancy is that the simulated result peaks at 28°, while the simulated results not only peaks at 27°. The measured results also has low signal in the 28° area, Also, if all of the measurements in Figure 5.2 are considered signal, the band in which signal is seen is much larger than that of the simulations. Alternatively, if the signal around 20° were to be considered background, then the range in which signal is measured experimentally is less than 5°, significantly less than the over 10° range from simulations.

This problem could come from multiple different issues. The most notable of while is the signal to noise present in the experimental measurement shown in

Figure 5.2. The error bars on each measurement are significant compared to the plotted average value. While repeated measurements in the form of the second pass do correlate well, such large error compared to signal makes the results questionable. What measurements can be considered background noise and which cannot is ill-determined.

There is also the possibility that the results from the simulation will not be as closely related to the experimental results as previously expected. PCgrate was shown to display the same overall behavior as experimental measures for experiments made in Littrow. However, no experimental results were available to compare to when there was a large angular deviation between the incident and reflected light. The discrepancy between the simulated and experimental measures could be due simply to an inaccurate simulation.

Another significant error source could be the input parameters of the simulation. The use of PCgrate requires accurate knowledge of the exact dimensions of the diffraction grating. The blazed angle of the grating was thought to be known to within a degree, however if this were not true the grating shape could change significantly.

The final possibility for the inconsistent measurements is the inconsistency of experimental data over long periods of time. The bolometer used for taking measurements has had numerous issues, including noise increasing over the span of a single set of measurements, as well as an inability to obtain identical

results between different sets of measurements on different cooling cycles. When more measurements can be made in a reliable manner the differences bet

6. **Future Work**:

Significantly more experiments need to be made and compared with simulated results. The consistency between the 150 GHz measurements and simulations is hard to determine due to the errors involved. More measurements for this particular grating need to be made to help lessen the impact of error. This will hopefully give results that we can have more confidence in. This reduction in error can also be found by using gratings that have higher signal. The 250 GHz and 410 GHz grating have significantly higher signal to noise during experimentation, and these may agree more closely with simulation, giving us a baseline for what we can expect for the relationship between the simulation and experiment. However, high angular resolution measurements with these gratings are not yet available.

Bibliography:

Goray, Leonid I. "Modified integral method for weak convergence problems of light scatting relief grating." Preceedings of SPIE (2001): Vol. 4291.

Loewen, E G, M Neviere and D Maystre. "Grating efficiency theory as it applies to blazed and holographic gratings." Applied Optics (1977): Vol. 16, No. 10.

Petit, R. Electromagnetic Theory of Gratings. Berlin Heidelberg New York: Springer-Verlag, 1980.

Thorlabs, Ruled Diffraction Gratings. 30th January 2014 <http://www.thorlabs.com/newgrouppage9.cfm?objectgroup_id=26>.

Appendix: A1:

This section includes additional comparisons between PCgrate and the gratings tests by Thorlabs.

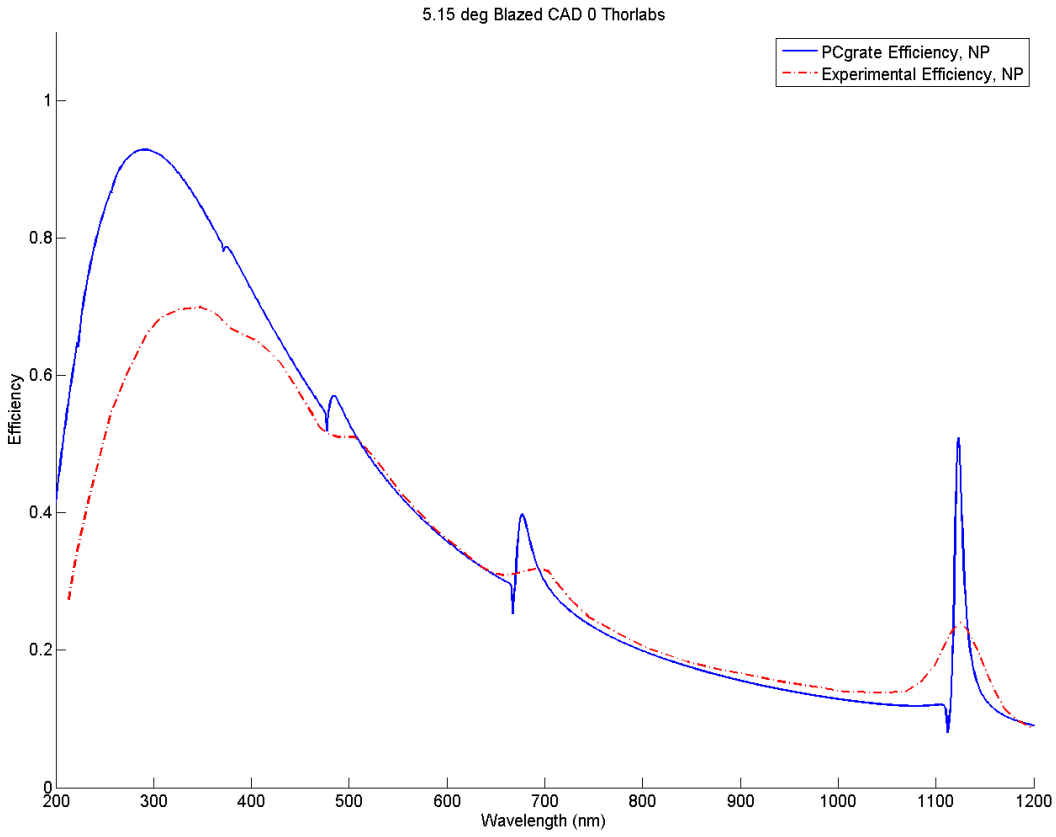

Figure A1.1: plot of the Efficiency of non-polarized (NP) for the grating for both an experimental measurement (in green) and the theoretical prediction from PCgrate (in blue). The grating is question is an upper right triangle with a blazed angle of 5.15° and a grove frequency of 600 groves/mm. Measurements were done in Littrow, where the constant angular deviation (CAD) is 0, for the -1 order (Thorlabs, Ruled Diffraction Gratings).

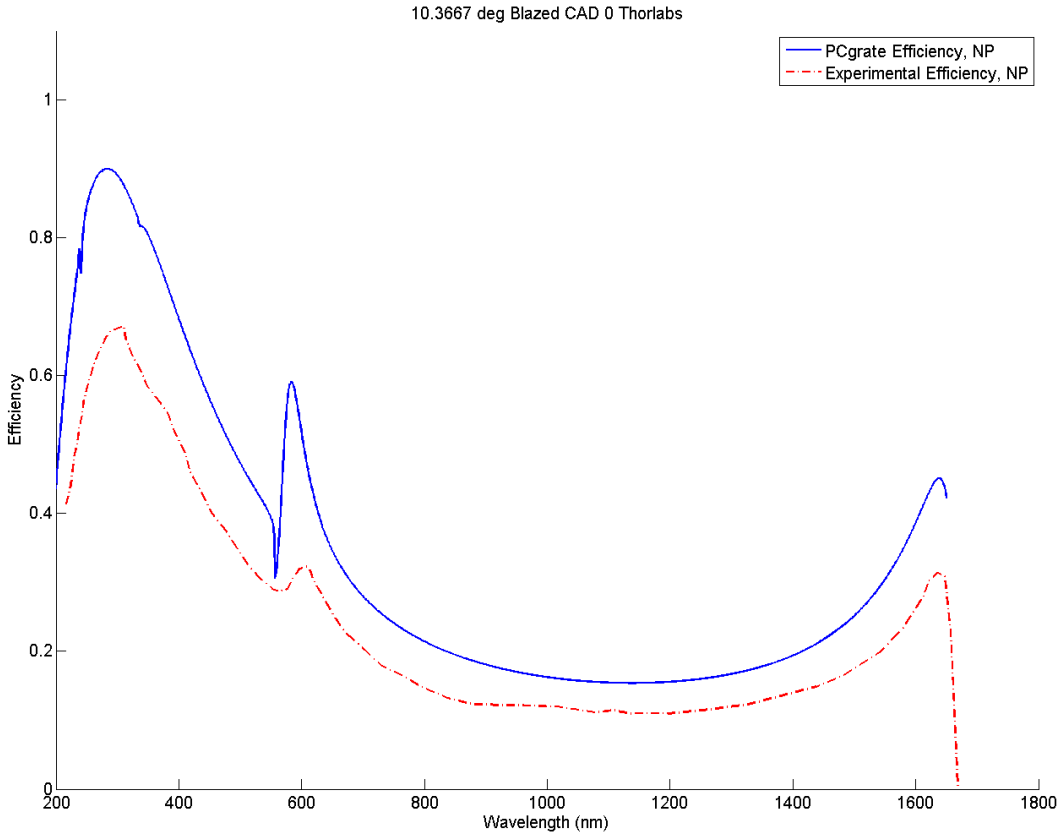

Figure A1.2: plot of the Efficiency of non-polarized (NP) for the grating for both an experimental measurement (in green) and the theoretical prediction from PCgrate (in blue). The grating is question is an upper right triangle with a blazed angle of 10.3667° and a grove frequency of 1200 groves/mm. Measurements were done in Littrow for the -1 order (Thorlabs, Ruled Diffraction Gratings).

Appendix: A2:

This section contains the additional plots of grating efficiency for the 250 GHz and the 410 GHz gratings as well as the spectral response of the filters used with these gratings. The final two plots of those of the 250 GHz and 410 GHz measurements taking all factors into account.

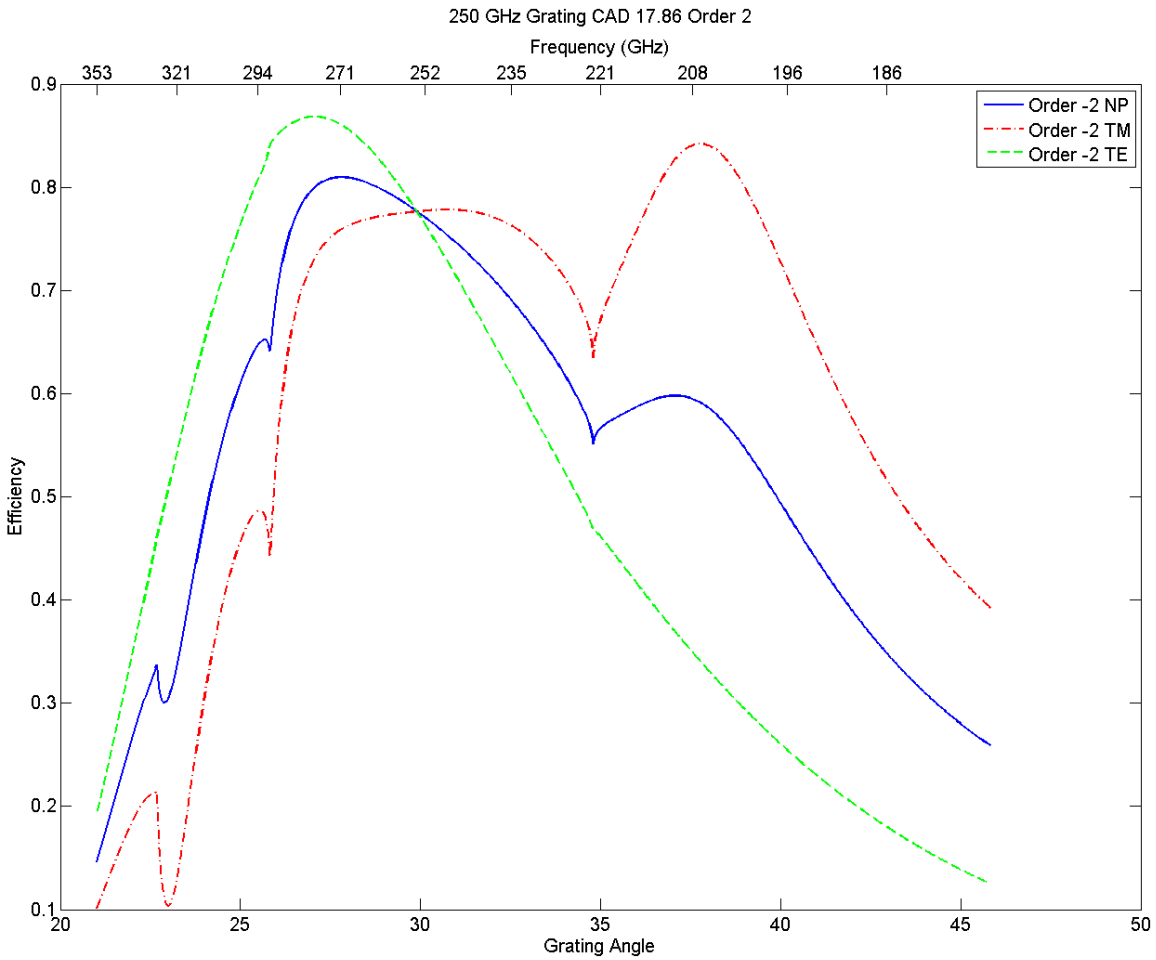

Figure A2.1: the efficiency of the 250 GHz grating. The grating efficiency is calculated for the second order (-2) and is shown in terms of the polarizations. The efficiency of Order -2 TE is that of light parallel to the groves of the grating, while the TM polarization is perpendicular to the groves.

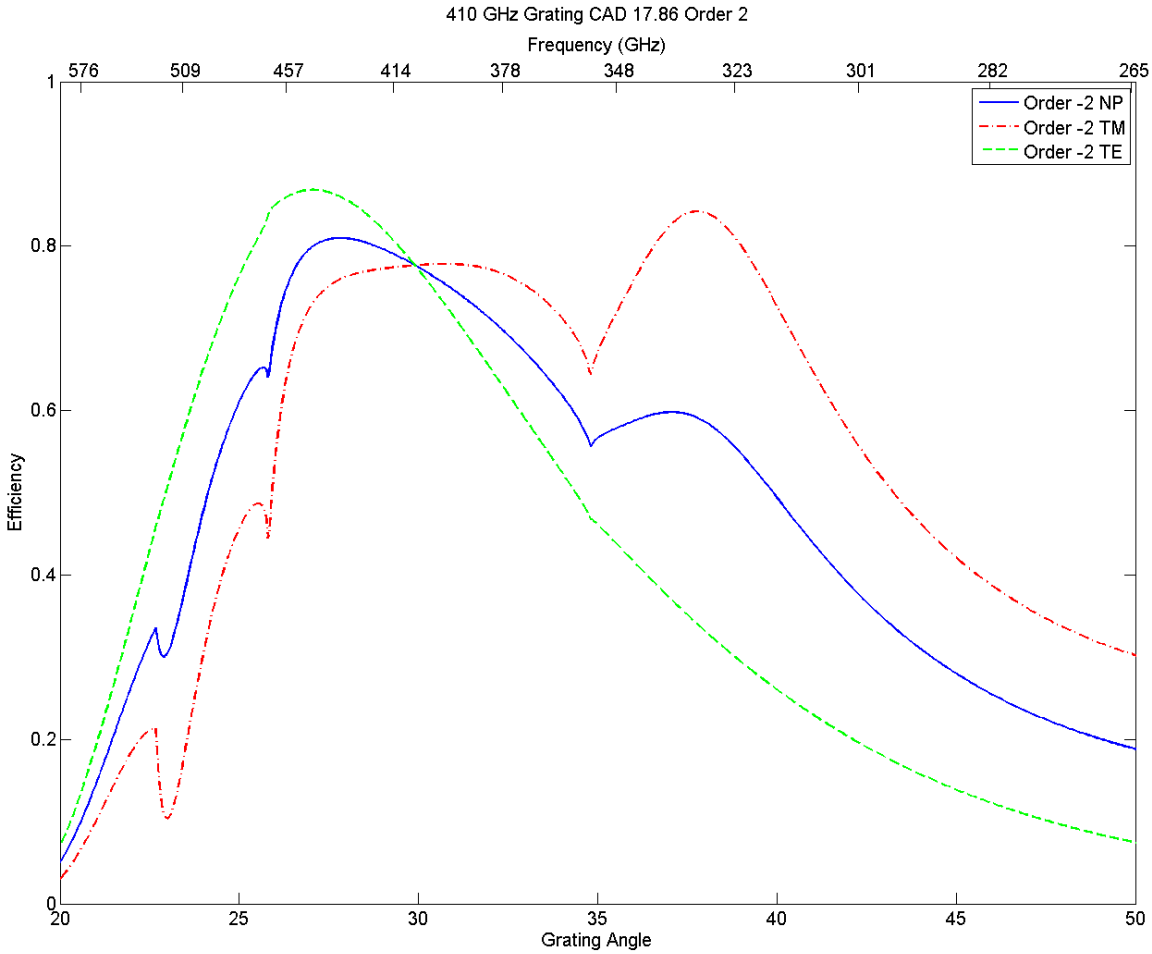

Figure A2.2: the efficiency of the 450 GHz grating. The grating efficiency is calculated for the second order (-2) and is shown in terms of the polarizations. The efficiency of TE is that of light parallel to the groves of the grating, while the TM polarization is perpendicular to the groves.

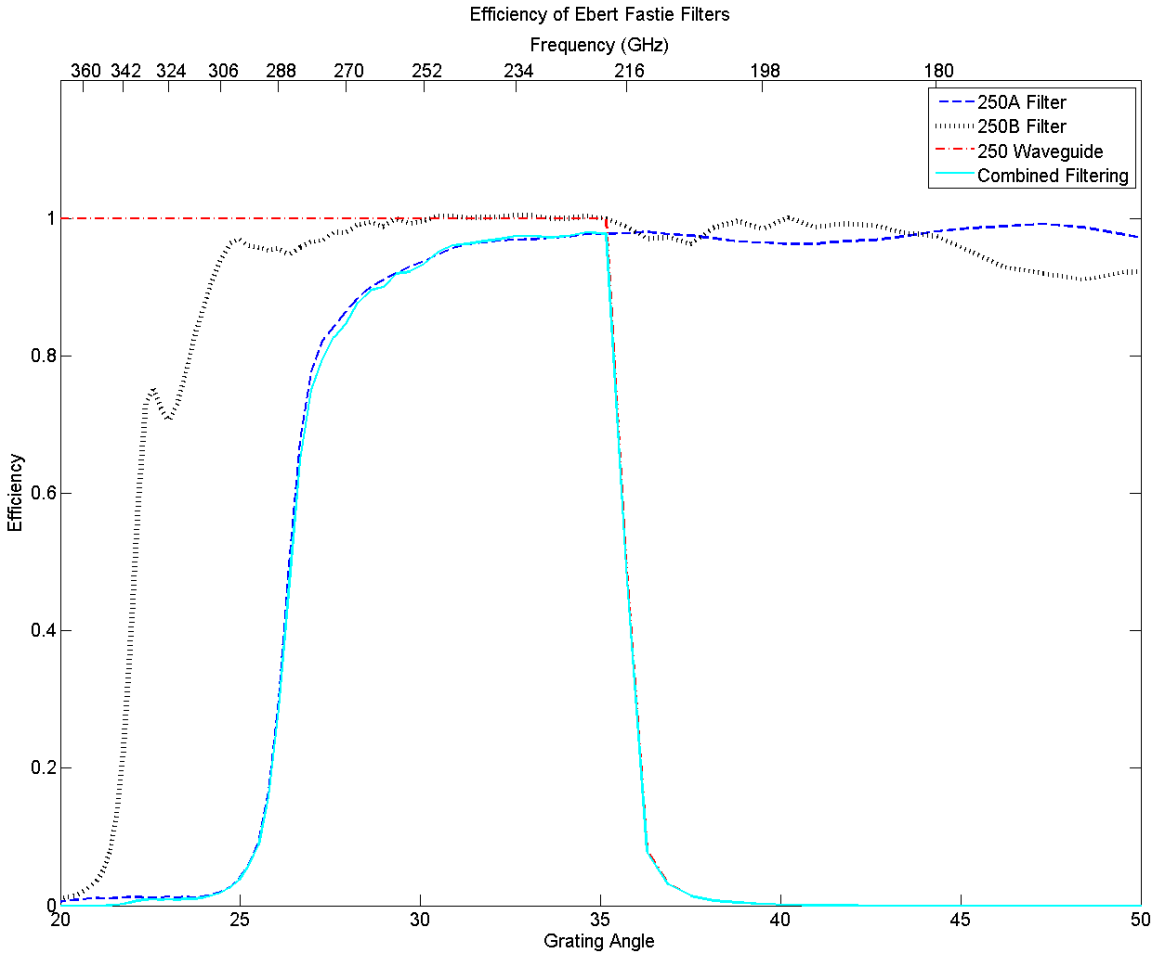

Figure A2.3: the transmission efficiency of each filter used in the 250 GHz measurement. Filters 250A and 250B are copper mesh filters, while 150 waveguide is an aluminum waveguide.

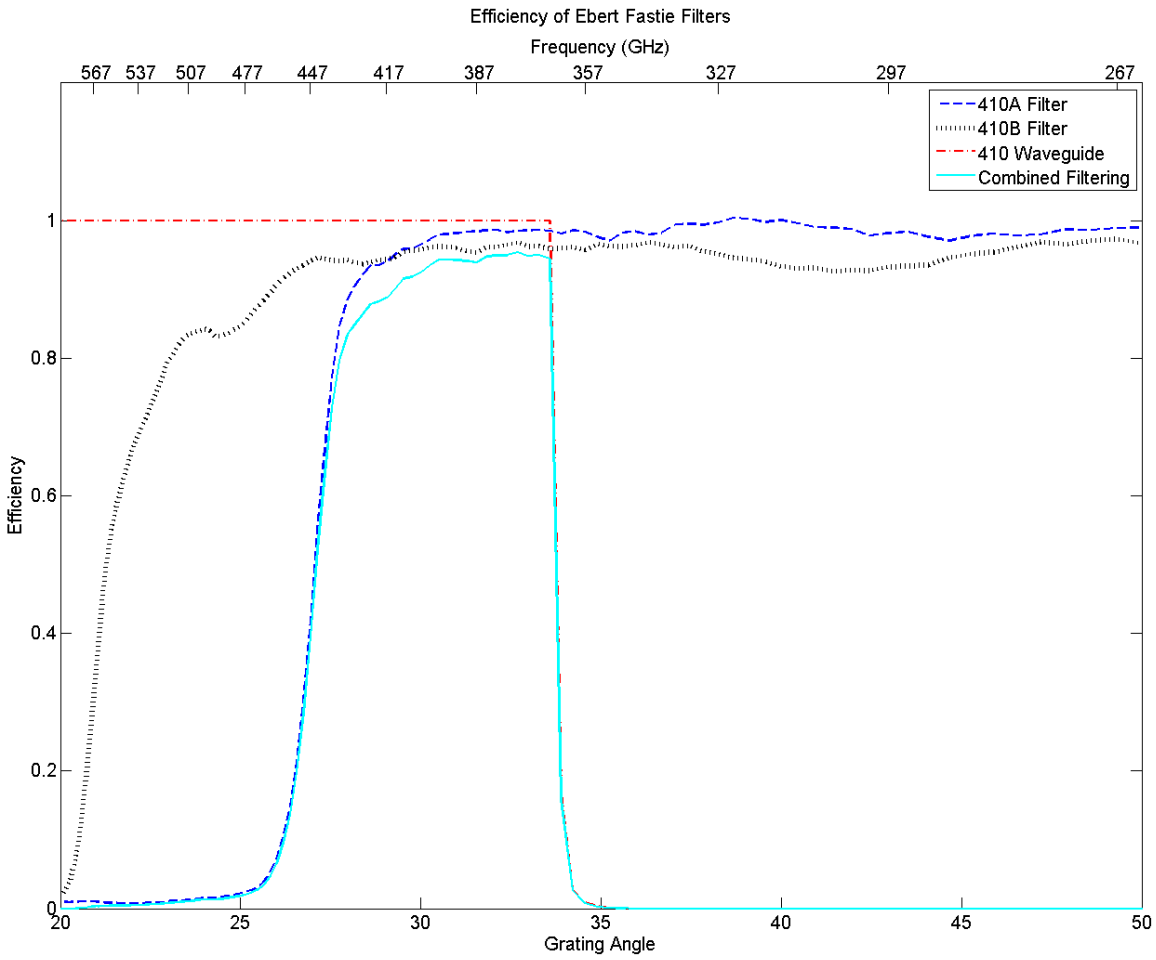

Figure A2.4: the transmission efficiency of each filter used in the 250 GHz measurement. Filters 250A and 250B are copper mesh filters, while 150 waveguide is an aluminum waveguide

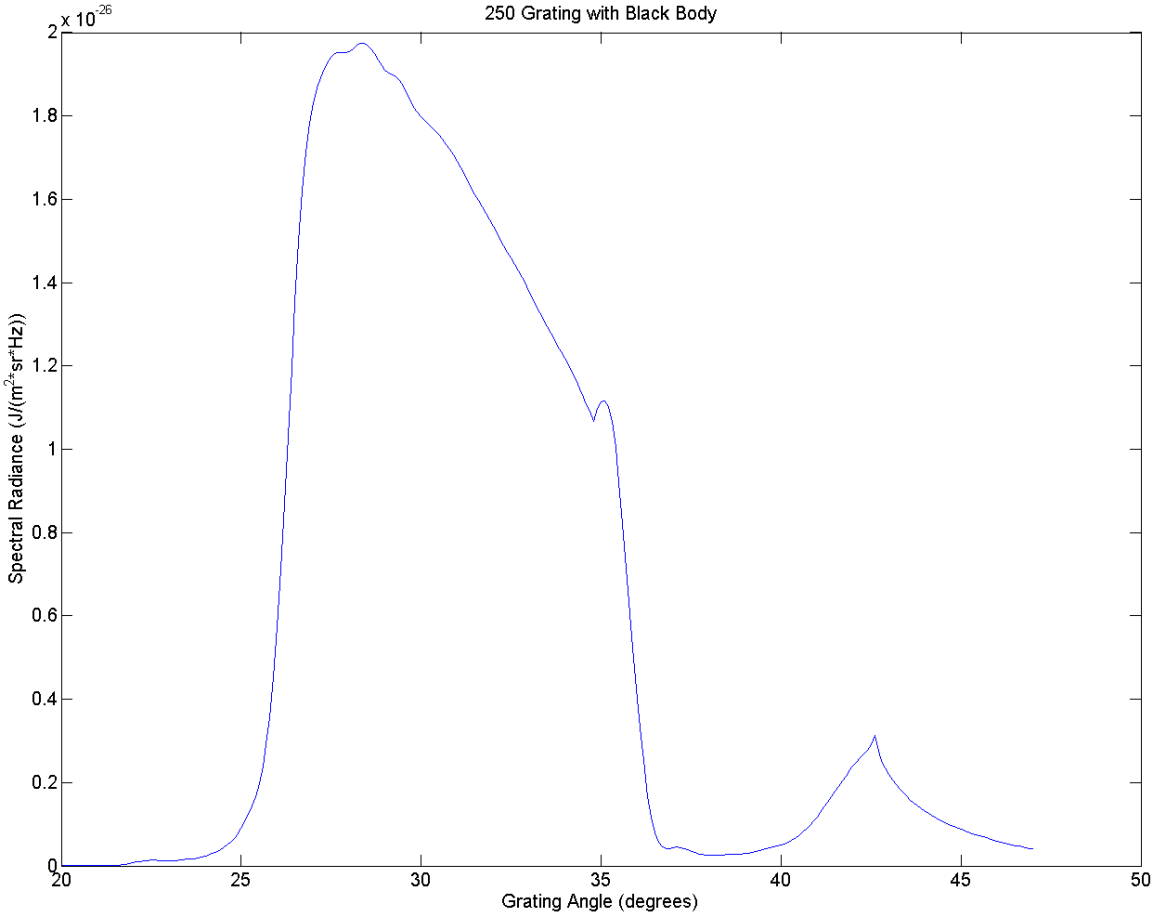

Figure A2.5: theoretical spectral response of the Ebert-Fastie with 250 GHz grating and filters including orders 1-15. This includes the blackbody, diffraction grating, high pass filters, low pass filters, and detector window.

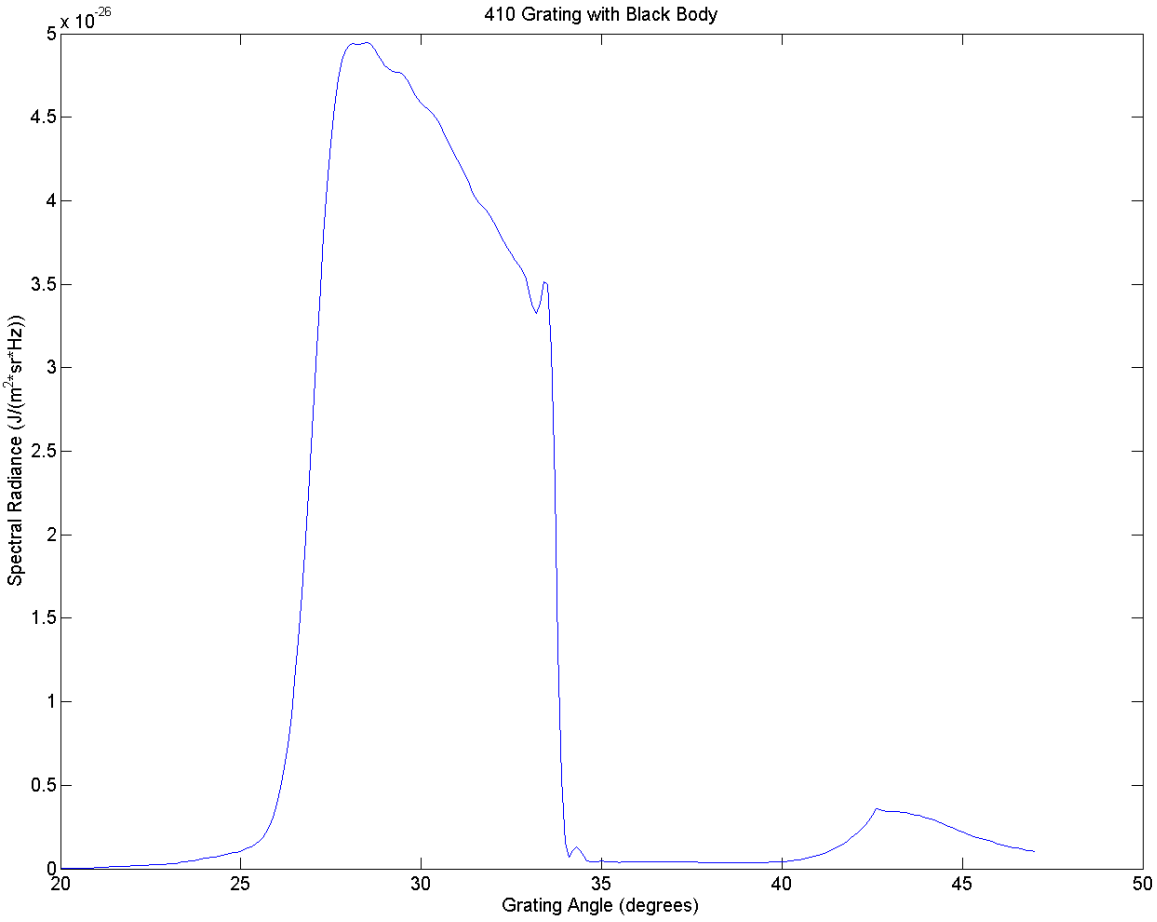

Figure A2.5: theoretical spectral response of the Ebert-Fastie with the 410 GHz grating and filters including orders 1-15. This includes the blackbody, diffraction grating, high pass filters, low pass filters, and detector window.

Appendix: A3:

This section contains the orders 1-9 for the 150 GHz grating. The 250 GHz and 410 GHz gratings each behave in a similar manner.

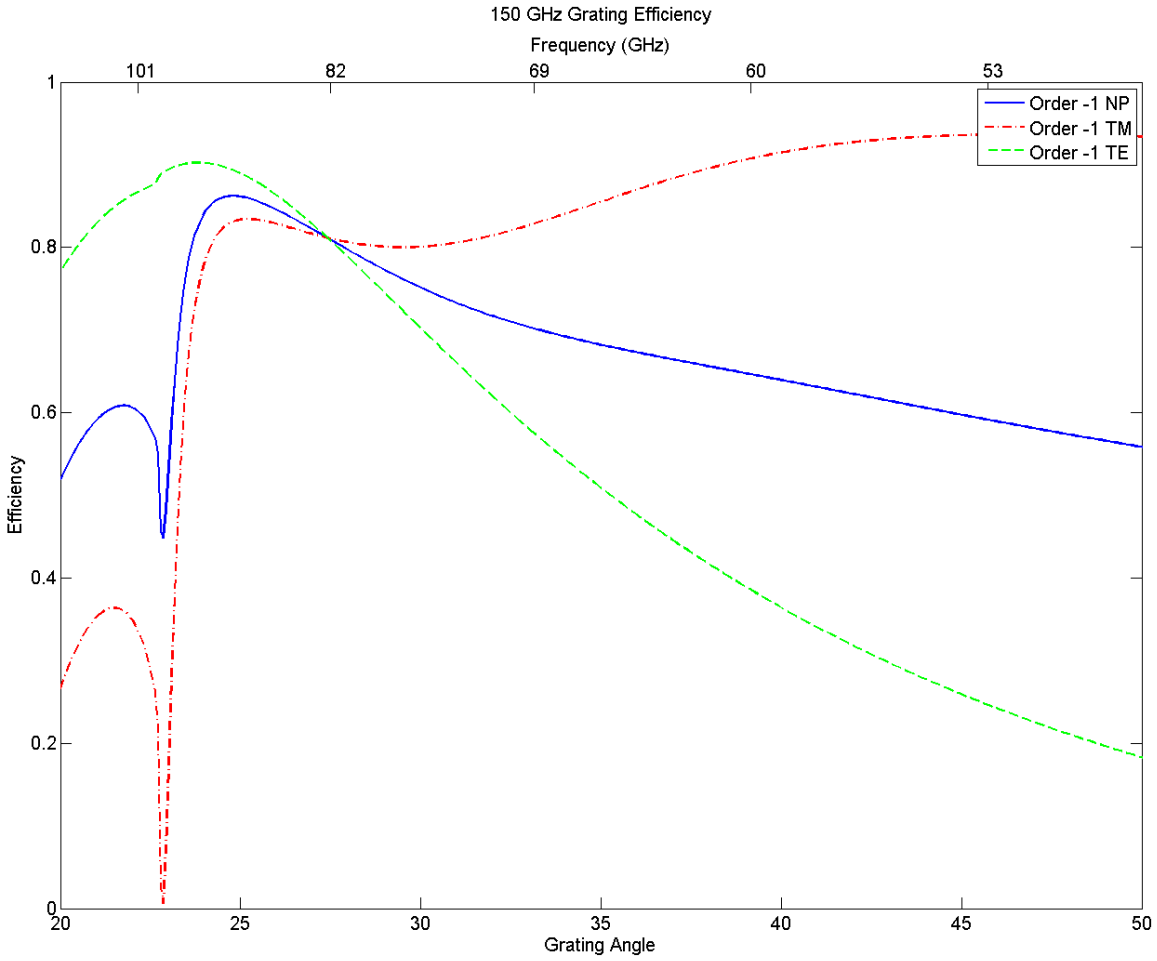

Figure A3.1: the efficiency of the 150 GHz grating. The grating efficiency is calculated for the first order (-1) and is shown in terms of the polarizations. The efficiency of TE is that of light parallel to the groves of the grating, while the TM polarization is perpendicular to the groves.

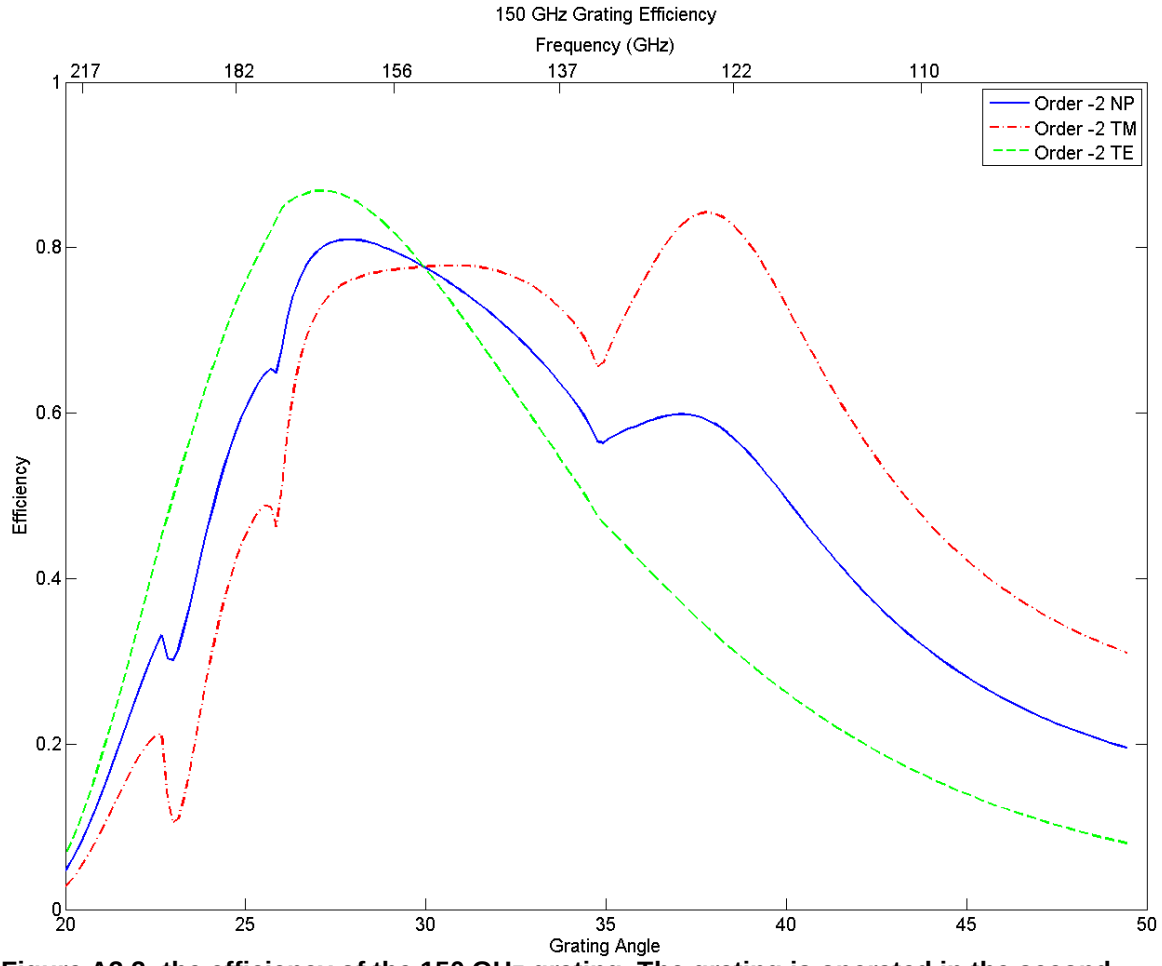

Figure A3.2: the efficiency of the 150 GHz grating. The grating is operated in the second order (-2) and is shown in terms of the polarizations. The efficiency of Order -2 TE is that of light parallel to the groves of the grating, while the TM polarization is perpendicular to the groves.

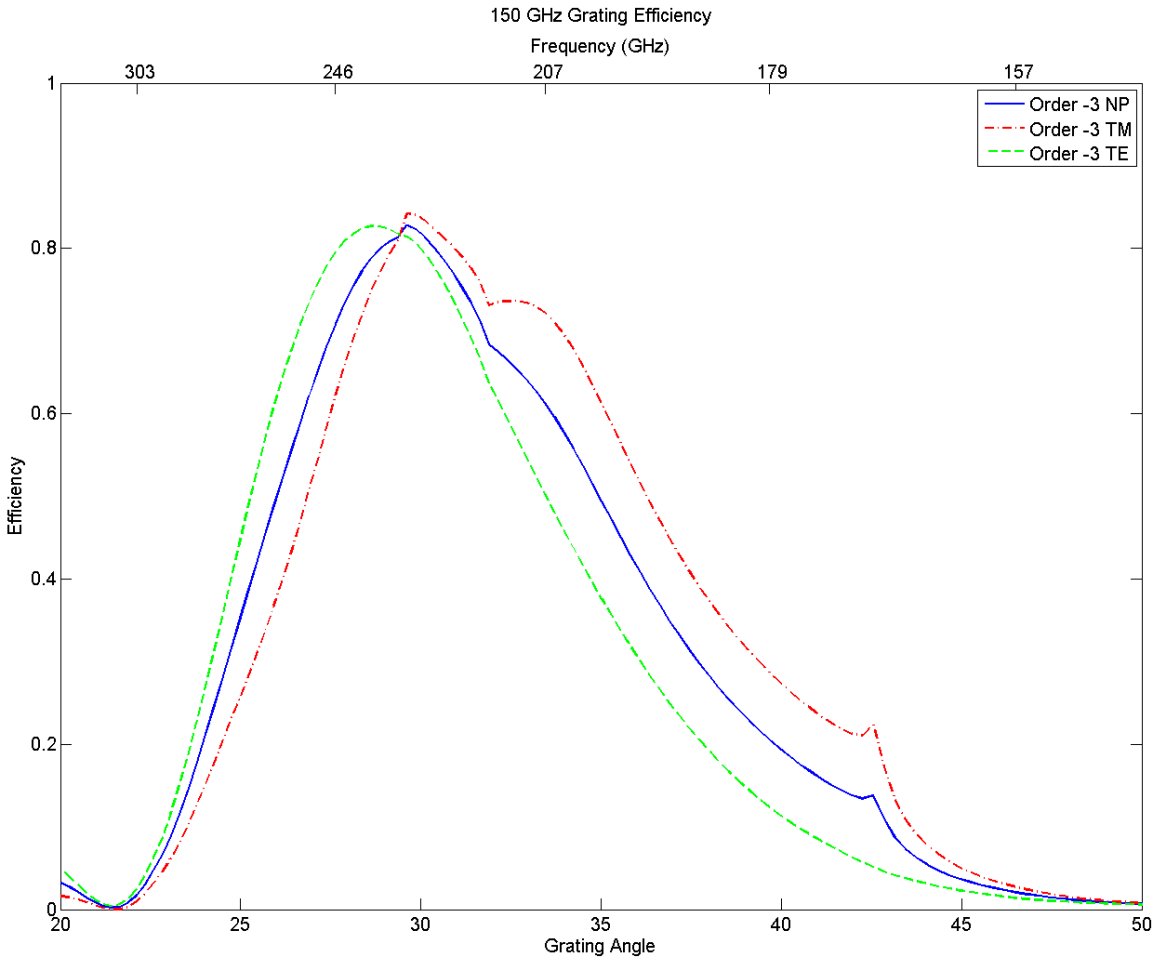

Figure A3.3: the efficiency of the 150 GHz grating. The grating efficiency is calculated for the third order (-3) and is shown in terms of the polarizations. The efficiency of TE is that of light parallel to the groves of the grating, while the TM polarization is perpendicular to the groves.

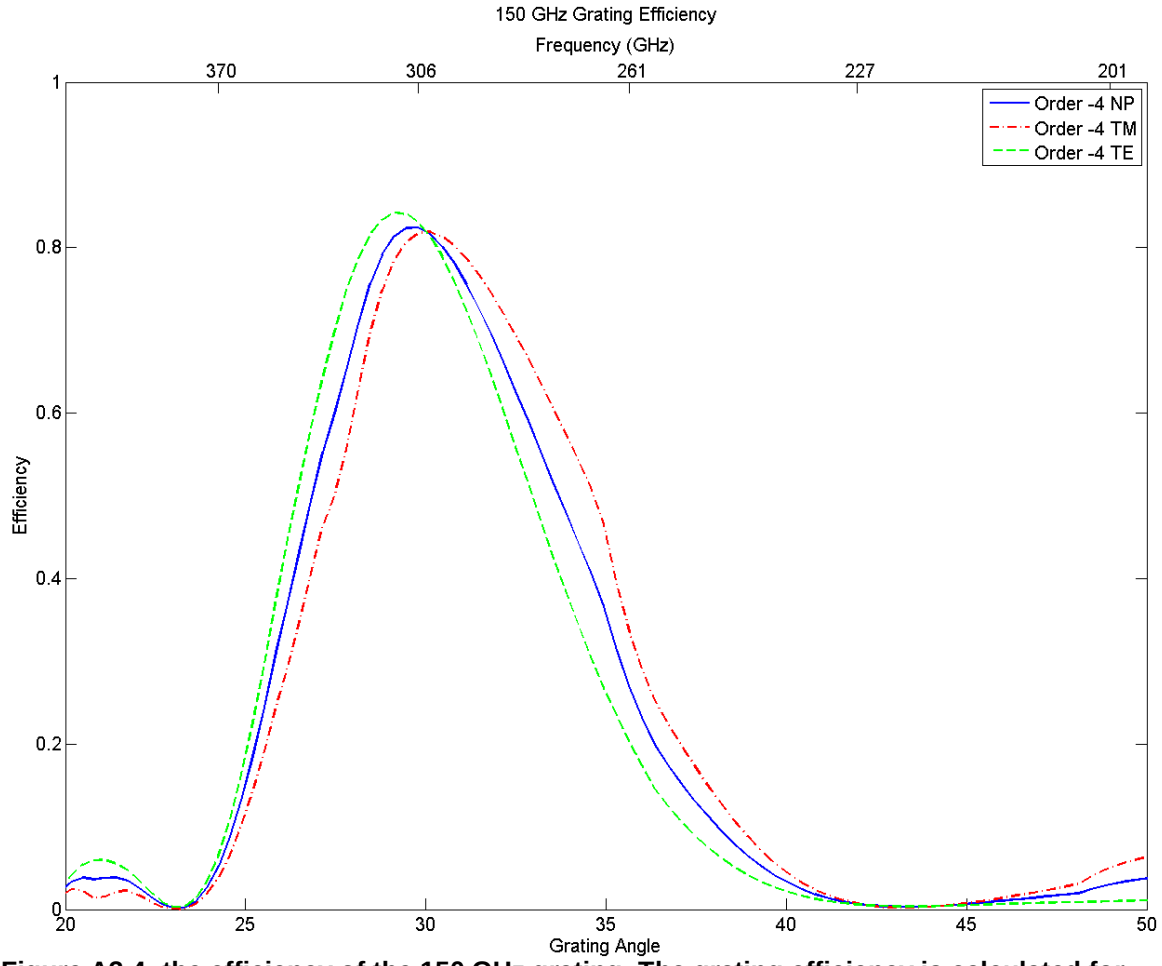

Figure A3.4: the efficiency of the 150 GHz grating. The grating efficiency is calculated for the fourth order (-4) and is shown in terms of the polarizations. The efficiency of TE is that of light parallel to the groves of the grating, while the TM polarization is perpendicular to the groves.

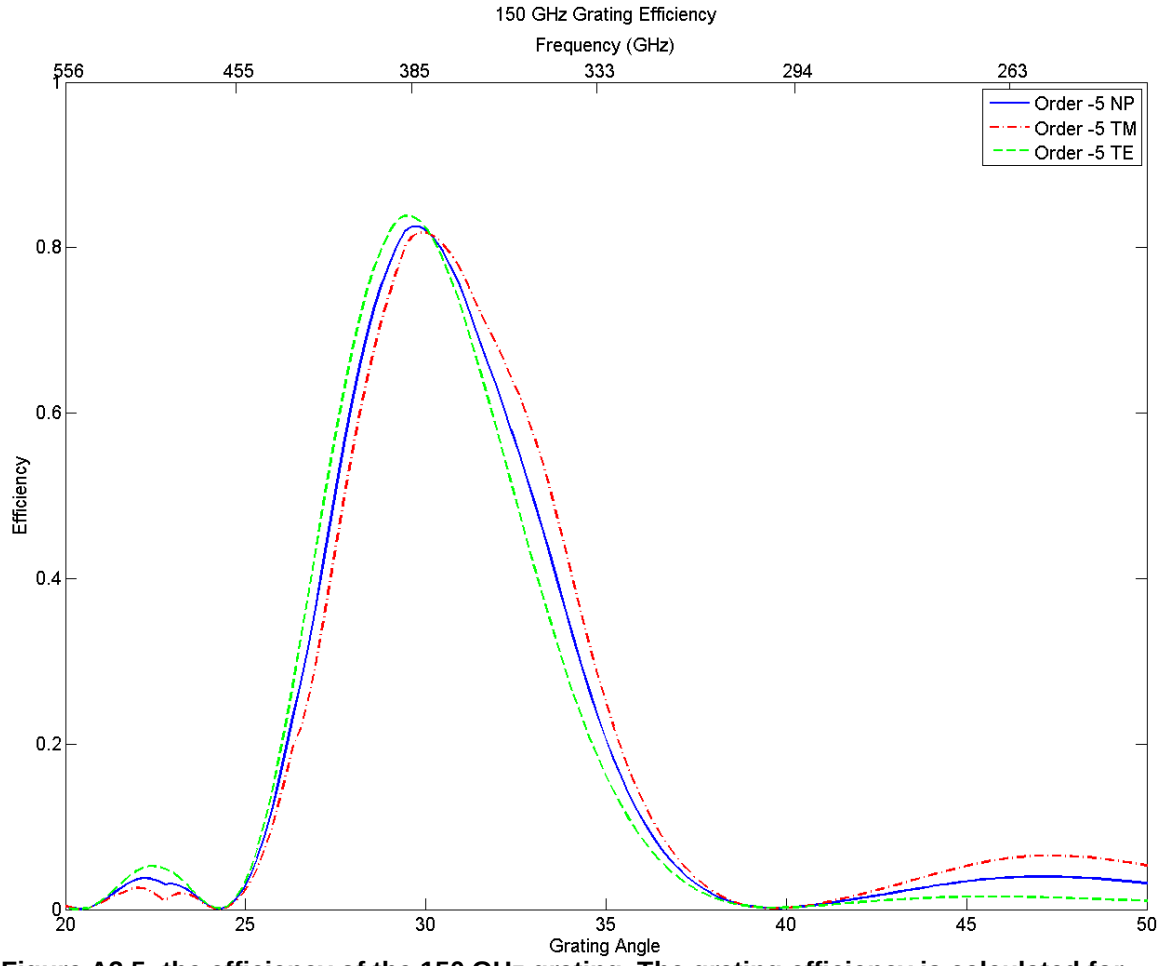

Figure A3.5: the efficiency of the 150 GHz grating. The grating efficiency is calculated for the fifth order (-5) and is shown in terms of the polarizations. The efficiency of TE is that of light parallel to the groves of the grating, while the TM polarization is perpendicular to the groves.

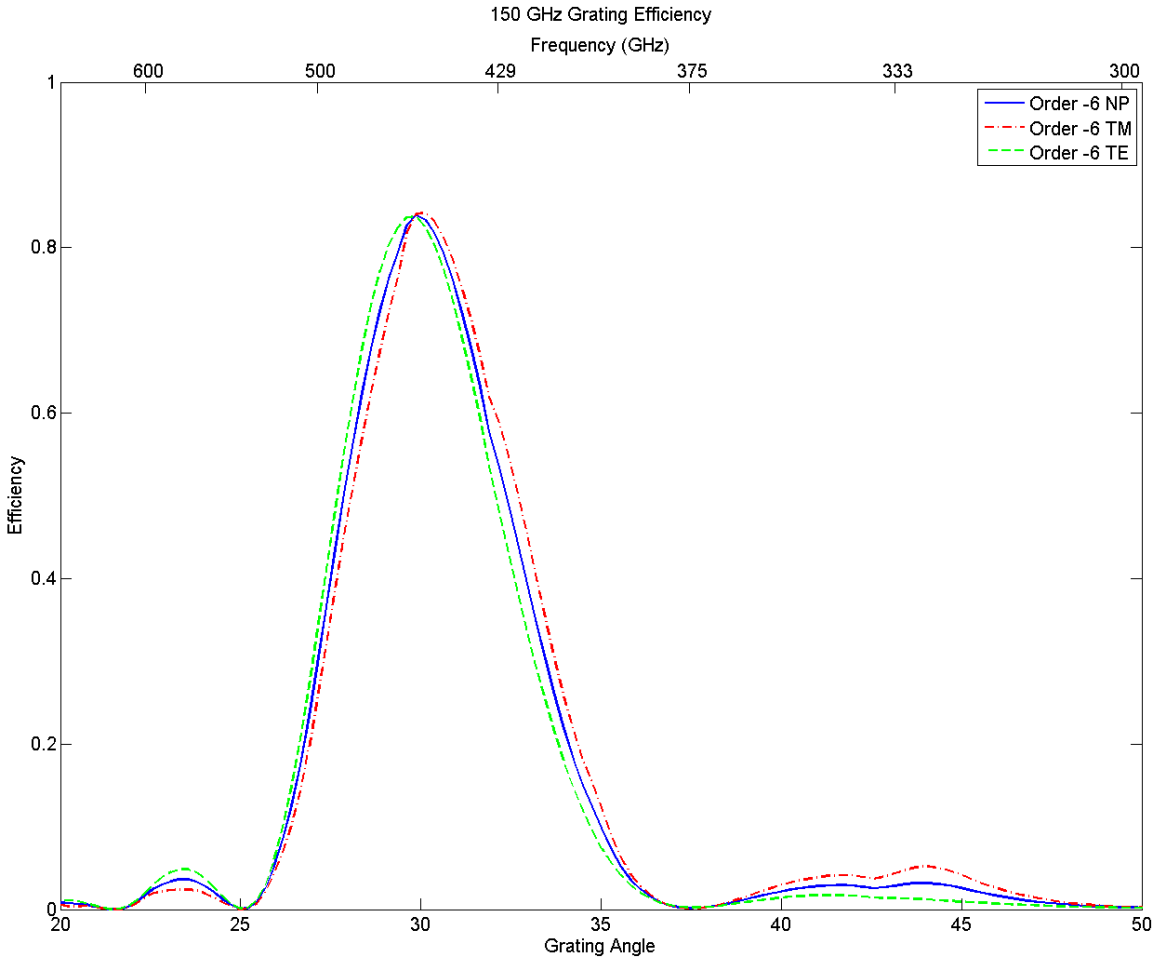

Figure A3.6: the efficiency of the 150 GHz grating. The grating efficiency is calculated for the sixth order (-6) and is shown in terms of the polarizations. The efficiency of TE is that of light parallel to the groves of the grating, while the TM polarization is perpendicular to the groves.

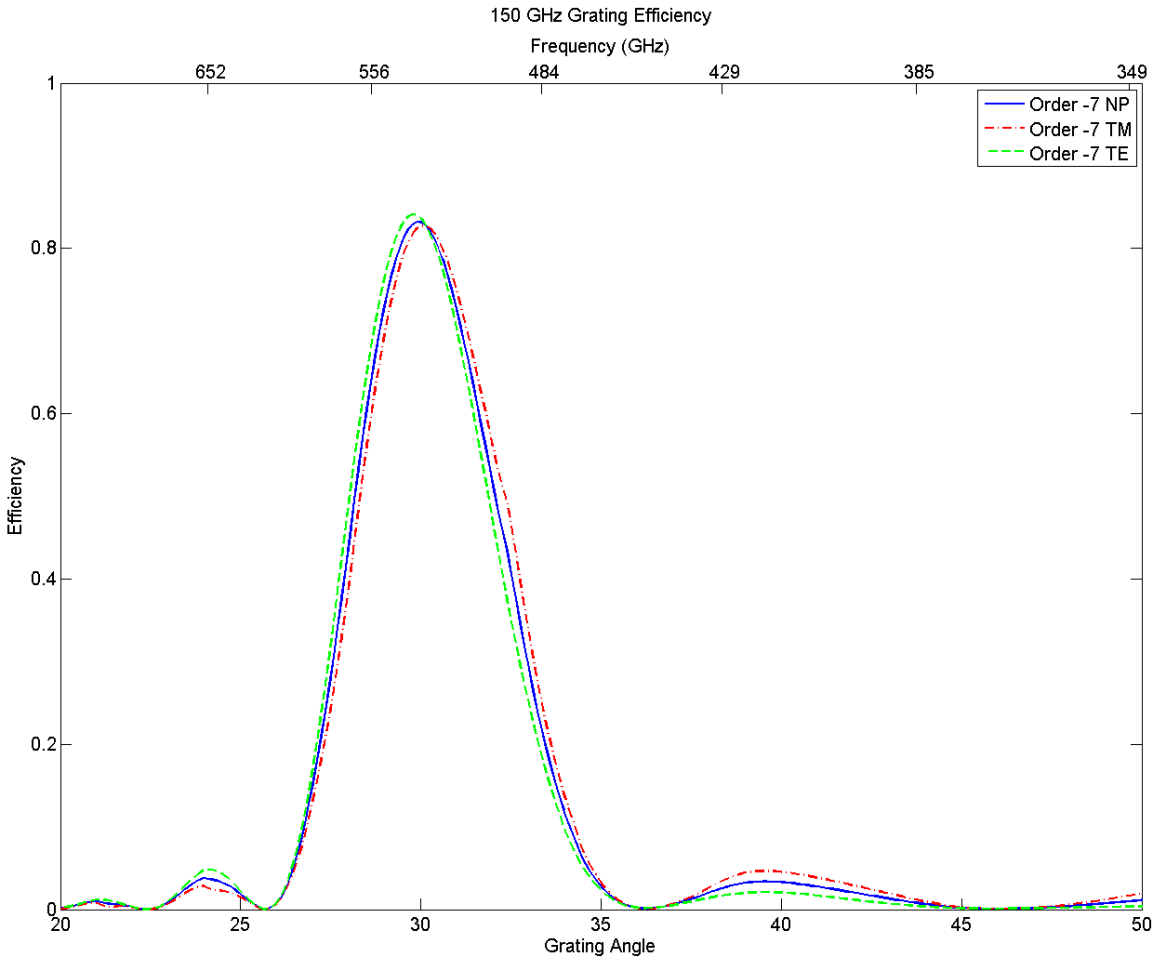

Figure A3.7: the efficiency of the 150 GHz grating. The grating efficiency is calculated for the seventh order (-7) and is shown in terms of the polarizations. The efficiency of TE is that of light parallel to the groves of the grating, while the TM polarization is perpendicular to the groves.

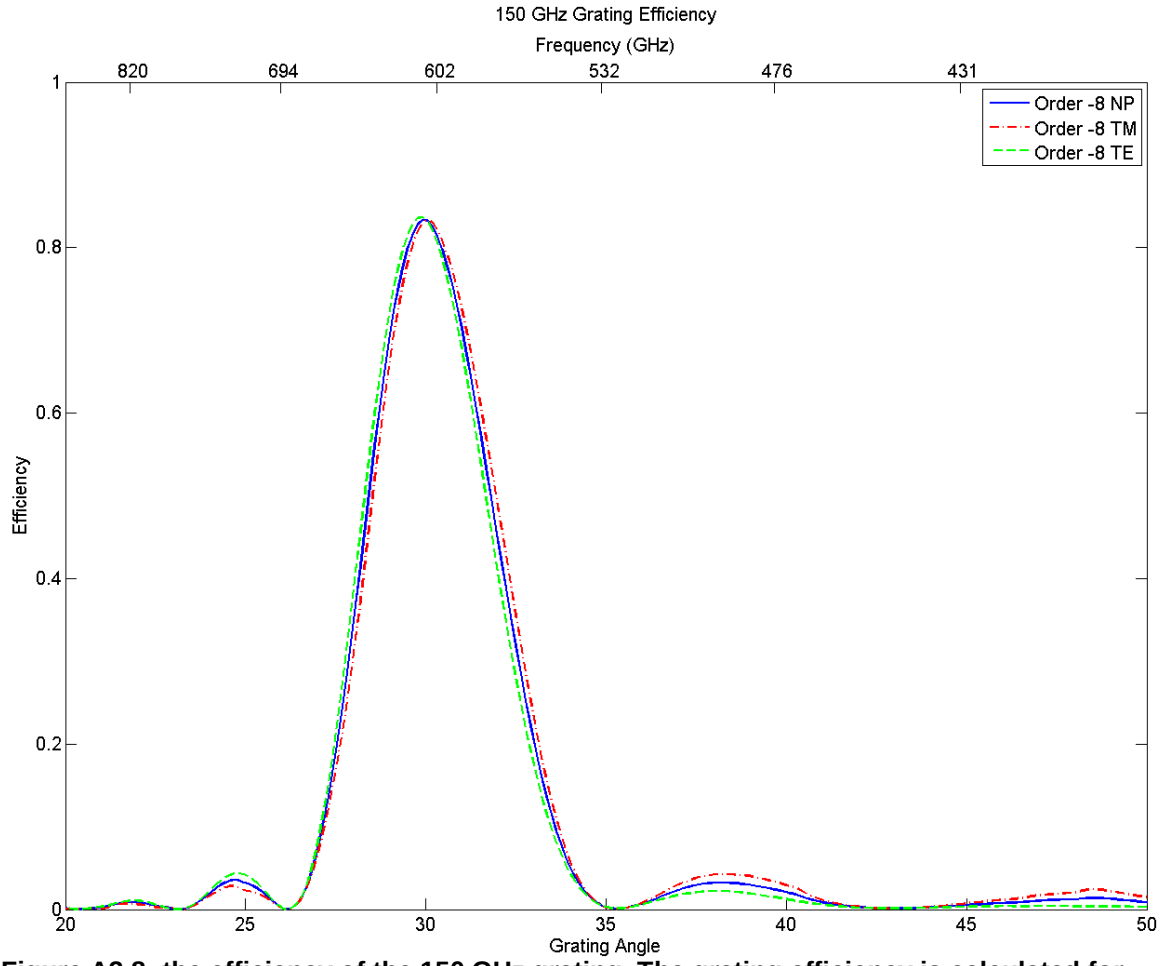

Figure A3.8: the efficiency of the 150 GHz grating. The grating efficiency is calculated for the eighth order (-8) and is shown in terms of the polarizations. The efficiency of TE is that of light parallel to the groves of the grating, while the TM polarization is perpendicular to the groves.

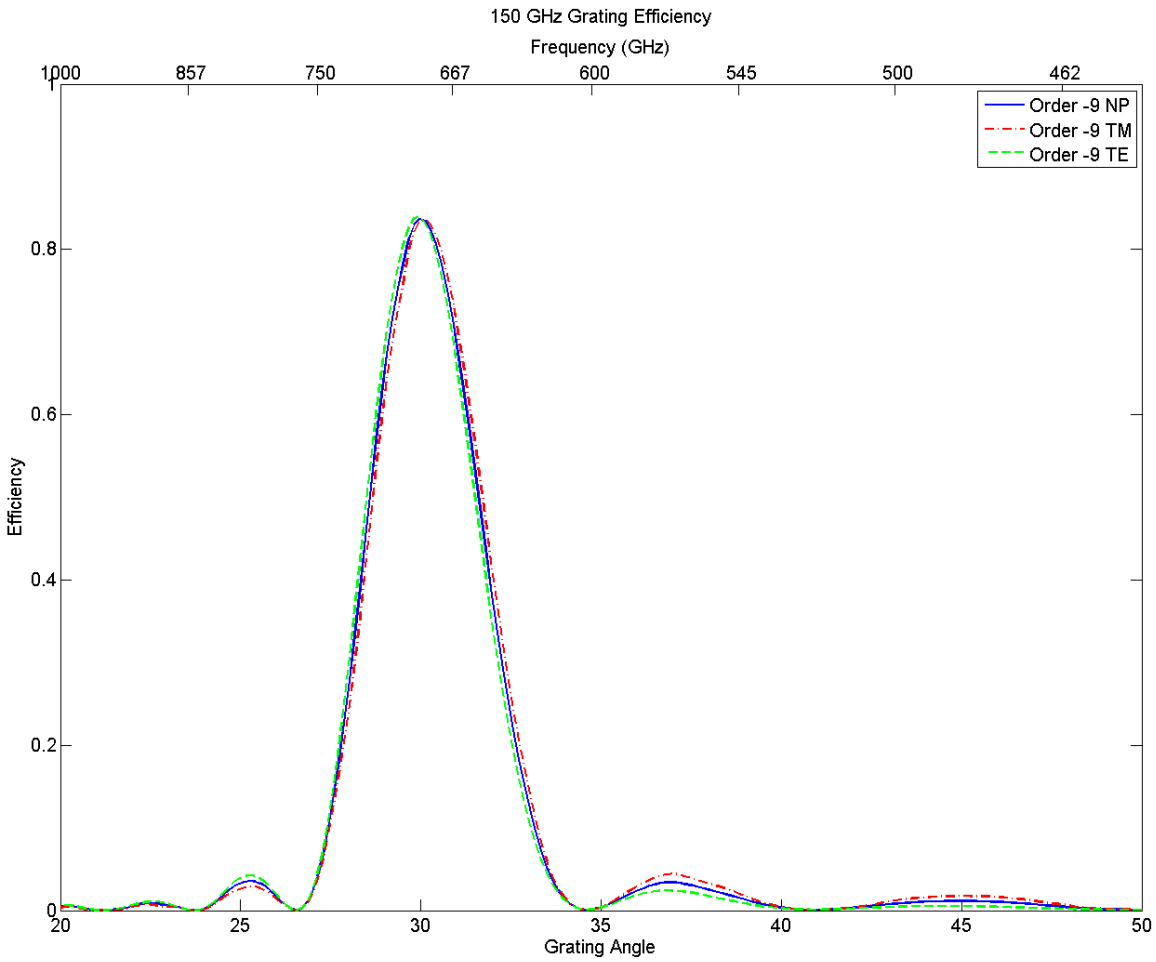

Figure A3.9: the efficiency of the 150 GHz grating. The grating efficiency is calculated for the ninth order (-9) and is shown in terms of the polarizations. The efficiency of TE is that of light parallel to the groves of the grating, while the TM polarization is perpendicular to the groves.